THE UNIVERSITY OF QUEENSLAND
AUSTRALIA
CREATE CHANGE

Overview of NERA research project: Converting tight contingent CSG resources: Application of graded particle injection in CSG stimulation

Presenter:
Dr Ray Johnson Jr
Professor of Well Engineering and Production Technology
UQ Centre for Natural Gas

Project contributors/researchers

UQ Centre for Natural Gas and its member companies (Arrow Energy, Australia Pacific LNG, Santos Ltd)

NERA (National Energy Resources Australia)

University of Queensland

- Dr Ray Johnson Jr and Dr Chris Leonardi, Co-Investigators
- Dr Zhenjiang You, Dr Ayrton Ribeiro, Dr Mohammad Sedgahat, Post-Doctoral Researchers
- Mr Nathan Di Vaira, Ms Vanessa Santiago, Ms Honja Ramanandraibe, Project PhD candidates

University of Adelaide

- Dr Alex Badalyan, Prof Pavel Bedrikovetsky, Dr Abbas Zeinijahromi, Dr Themis Carageorgos

University of Alberta

- Prof Rick Chalatyrnak, Francy Guerrero, Angel Sanchez, Dohyun Kim, Nathan Deisman, Jakob Brandl, and Kevin Hodder

Project Report/Presentation Structure

- Problem definition and background
- What we know and don't know
  - Hydraulic fracture modelling and limitations
  - Proppant transport, straining and embedment Behaviour
- What could success look like
  - Characterising pressure-dependent permeability behaviour in coal using an integrated approach
  - Reservoir simulation of GPA application single frac or multi-stage fracs
- How do we deploy it
  - Laboratory testing of fluids and commercially available micro-proppant
  - Development of well selection criteria for GPI implementation
- Conclusions and recommendations

Problem Definition

- GPI was first proposed as a technology to improve the poor production index observed in naturally fractured unconventional reservoirs such as coal seams (Keshavarz, et al., 2015; Keshavarz, et al., 2016; Alireza Keshavarz, et al., 2014; Khanna, et al., 2013)
- Laboratory testing methodology was created to predict productivity responses of GPI in the SRV

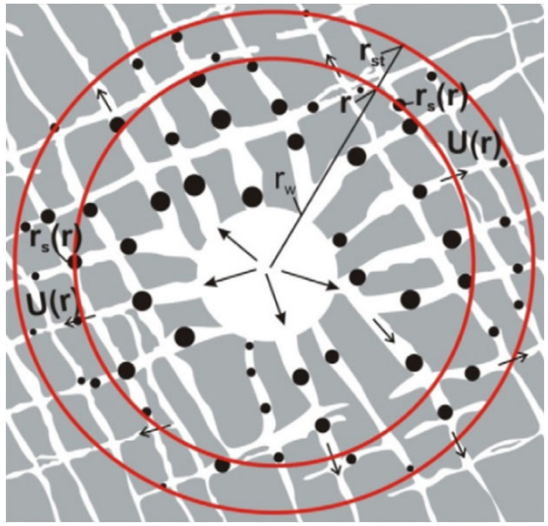

Figure 1

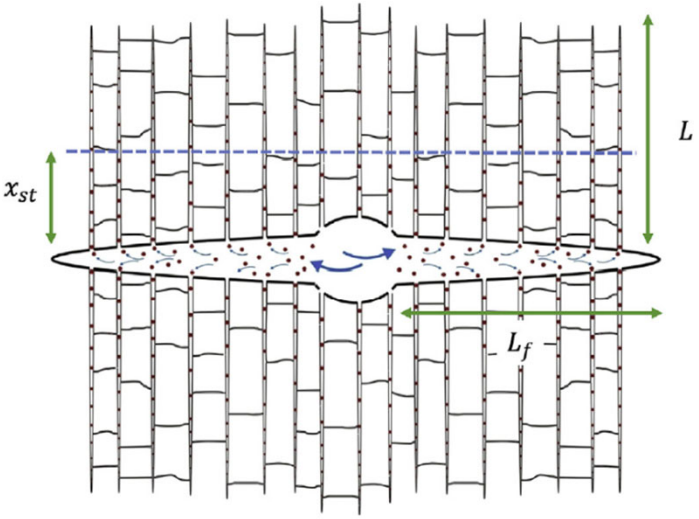

Figure 2

Schematic representations of graded particle injection, showing (**Figure 1**) the relative movement of particles of increasing size (reproduced from Keshavarz et al., 2014) and (**Figure 2**) its application in conjunction with hydraulic fracturing (reproduced from Keshavarz et al., 2016).

Problem Definition

- Micro-proppants should enhance the simulated reservoir volume (SRV) created by early-time injections during frac that are unpropped using conventional proppants (**Figure 3**)
- Laboratory testing has created models we can use to predict productivity responses of the SRV (**Figure 4**)
  - Initial permeability k_i=0.37 mD
  - Increase $P_{injection}$ up to 900 psi and k up to 3.88 mD with clean fluid
  - Inject 5 mm proppant until C_D=0.241
  - Continue injection of proppant-free solution and reduce $P_{injection}$ down to 50 psi
  - Final permeability k_{cycle1}=0.9 mD
- Resulting improvement in SRV (k_{cycle1}/ k_i) is 2.43

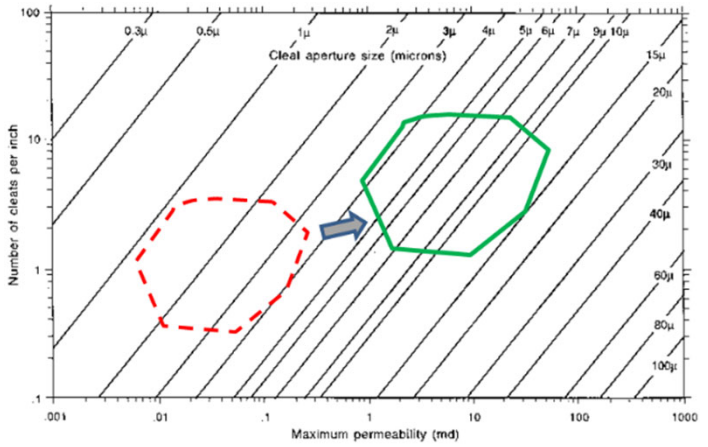

Figure 3 (Modified after Laubach, S.E. et al., 1998)

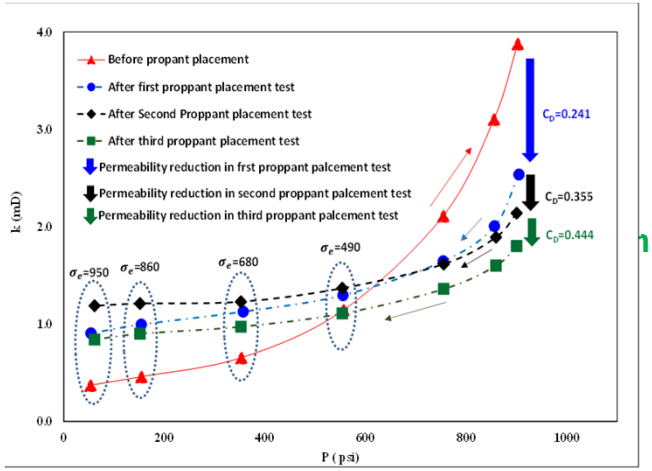

Figure 4 (After Keshavarz, et al., SPE-182306-MS, 2016)

Hydraulic Fracture Modelling and Limitations

- Australian studies have noted that non-planar components are more widespread in the Australian stress environment and represent a significant volume of the hydraulic fracture pumped within a coal stimulation treatment *(Badri, et al., 2000; Johnson Jr, et al., 2002; Morales & Davidson, 1993; Jeffrey, et al., 1992; Jeffrey & Settari, 1995, 1998; Jeffrey, et al., 1998; Johnson Jr, et al., 2021)*
- Despite significant diagnostic and modelling efforts, the non-planar components and the secondary benefits of non-planar fractures cannot be finely estimated to guide decisions regarding future treatment strategies *(Thomas Flottman, et al., 2013; Johnson Jr, Glassborow, et al., 2010; Johnson Jr, Scott, et al., 2010; Scott, et al., 2010; Megorden, et al., 2013; Ramanandraibe et al., 2022).*
- Hydraulic fracture simulators' inability to capture shear slip at weak interfaces and fracture crossing where contrasting low to high Young's modulus and vice versa *(Gu & Siebrits, 2006)* and constraining height based on shear slip at these weak interfaces *(Scott, et al., 2010; Pandey, et al., 2017)*
- As part of this study, a review was made of potential hydraulic fracture simulators capable of modelling GPI in a hydraulic fracture (Aghighi, et al., 2019) to identify the most logical model to:
  - incorporate the morphology of natural fractures and stress tensors in a three-dimensional finite element-discrete stress model;
  - model of microparticle suspensions which simultaneously bridge at scales at which colloidal and non-Brownian behaviours exist; and
  - provide framework in which the viscous, mechanical, inertial, electrostatic, and thermodynamic forces are relevant to the particle transport in porous and fractured media

PROPPANT TRANSPORT, STRAINING AND EMBEDMENT BEHAVIOUR (1)

- The modelling of proppant embedment, fracture conductivity, and production enhancement was improved from prior estimates of productivity for radial injection of GPI using three sub-models (You et al., 2019; Wang et al., 2021):
  - An elastoplastic finite element model is used to calculate the embedment depth and fracture deformation under varying particle packing density, effective stress and material parameters (You et al., 2019).
  - A fracture permeability model considering effective stress (σ_e) embedded particles using the coupled lattice Boltzmann-discrete element model (LBM-DEM) (Wang et al., 2021)
  - The productivity index after well stimulation by microparticle injection is performed using radial flow model with the fracture permeability
- Results consistent with StimLab studies showing increasing embedment with rank (Fraser and Johnson, 2018) with discernible shear failure and permeability detriment by fines generation

Figure 5: Embedment vs σ_e for Bowen Coal Example

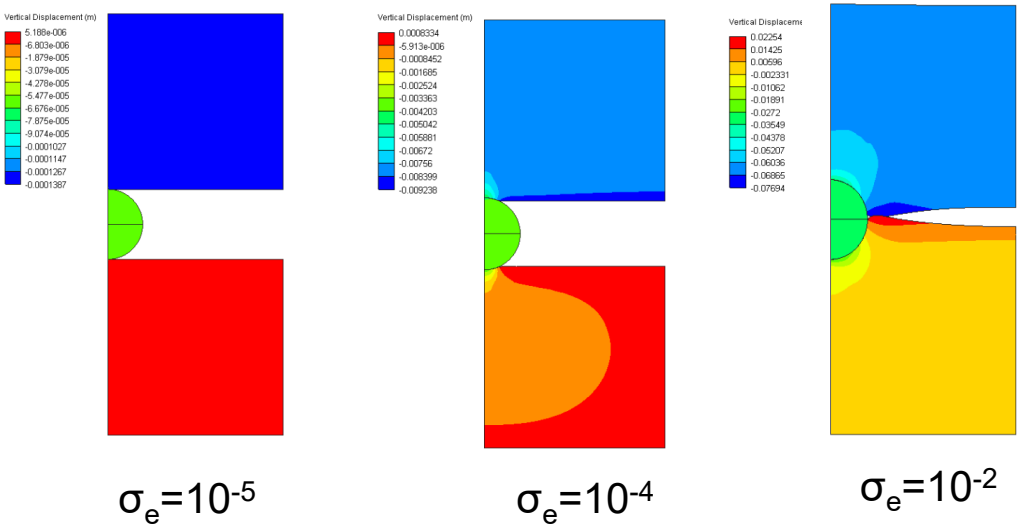

Figure 6: Embedment vs σ_e for Surat Coal Example

PROPPANT TRANSPORT, STRAINING AND EMBEDMENT BEHAVIOUR (2)

THE UNIVERSITY OF QUEENSLAND AUSTRALIA

Penetration Versus Productivity Increase

Figure 7 - Bowen Coal

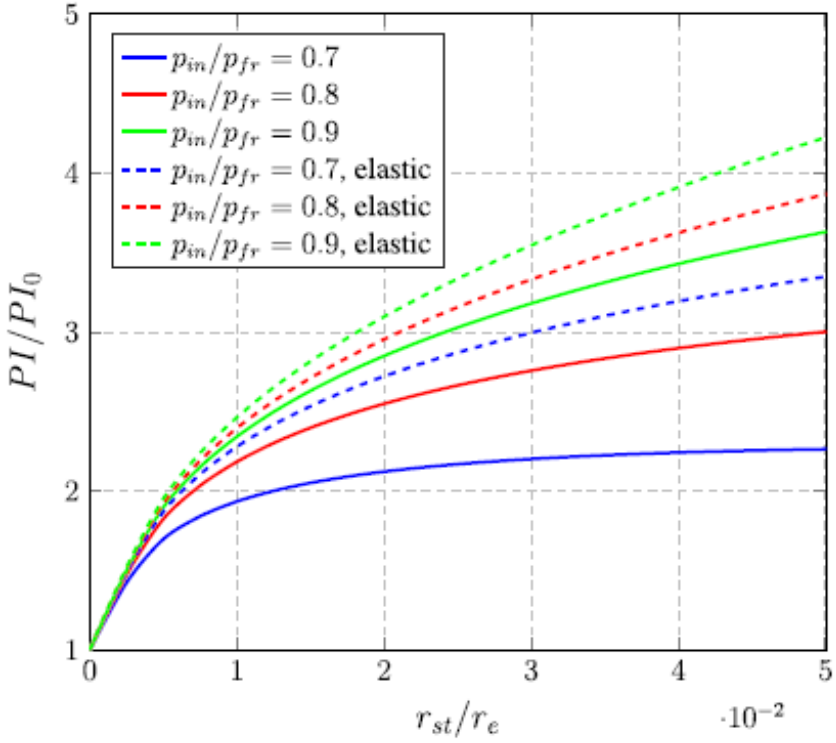

Figure 8 - Surat Coal

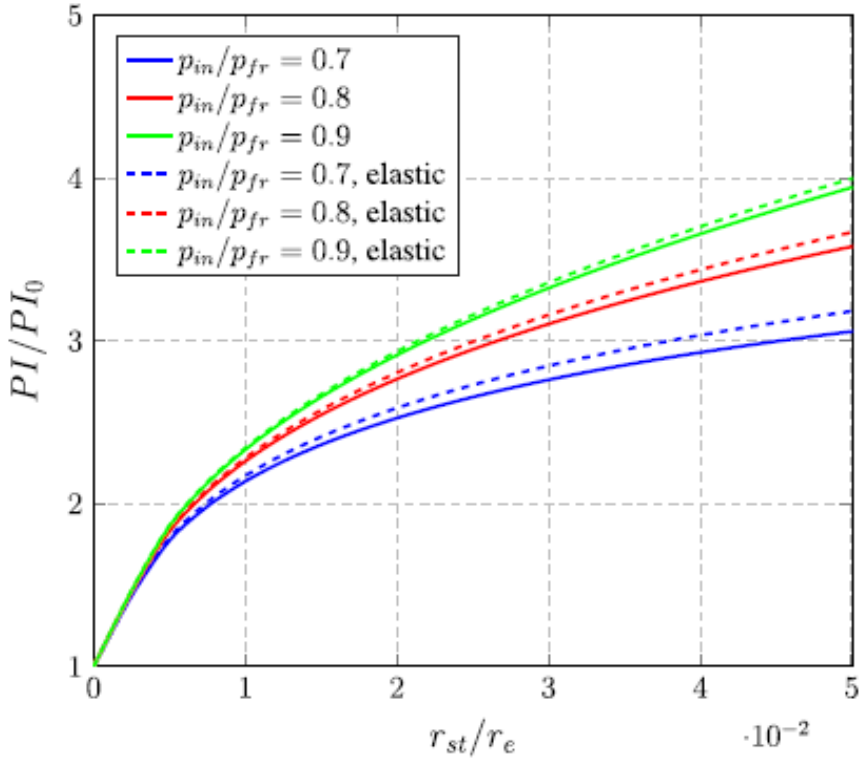

Using a radial model (see Figure 1) investigations were made relating to penetration and productivity increase varying injection pressure for both Bowen and Surat Basin Coals.

PROPPANT TRANSPORT, STRAINING AND EMBEDMENT BEHAVIOUR (3)

THE UNIVERSITY OF QUEENSLAND AUSTRALIA

Fracture Compressibility Versus Productivity

Figure 9 - Bowen Coal

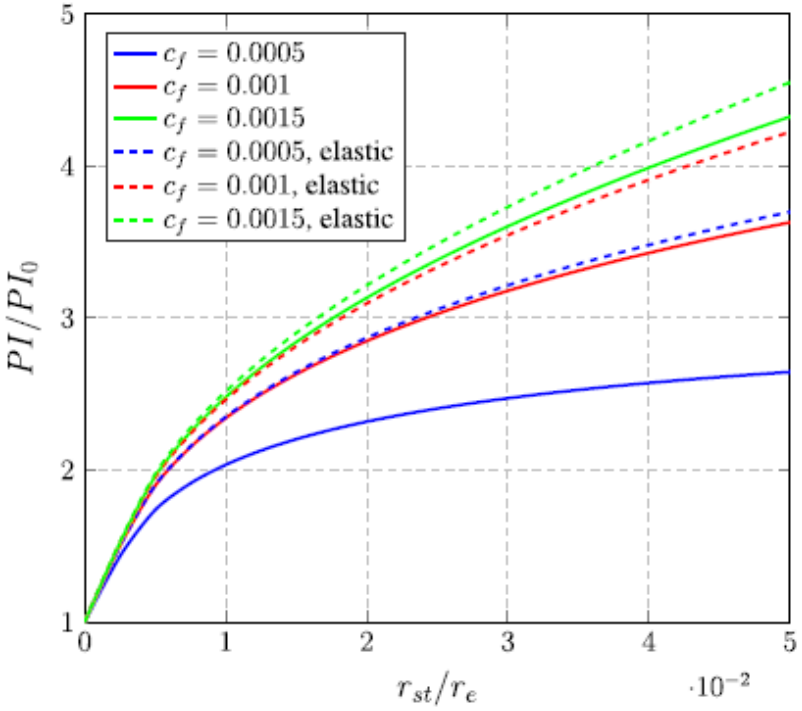

Figure 10 - Surat Coal

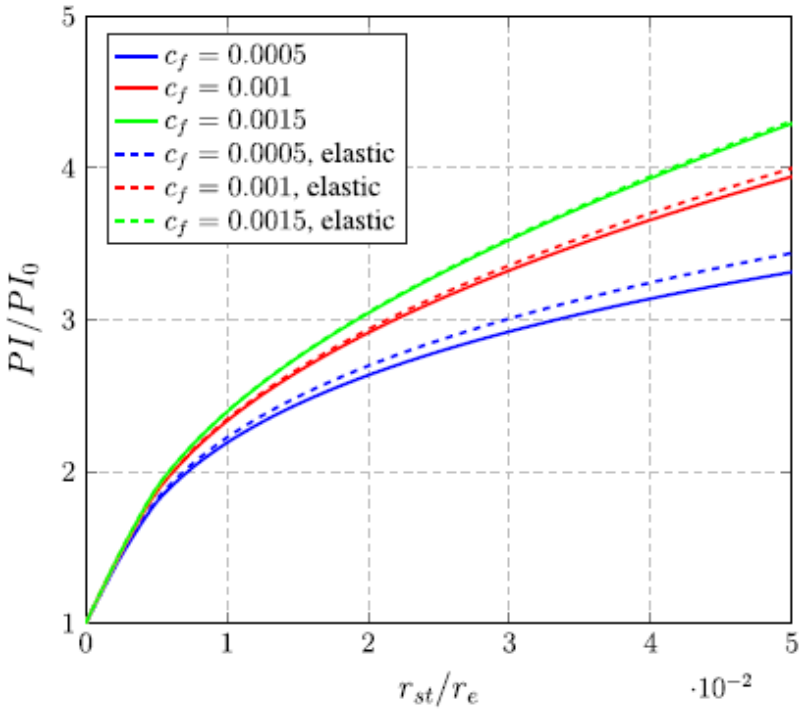

- Similarly, investigations were made relating to fracture compressibility (c_f) and productivity increase varying injection pressure for both Bowen and Surat Basin Coals.
- **Hence, a methodology to constrain c_f became an objective of the study**

Results- Sand conductivity vs coal thermal maturity

- Mount Compass sourced 20/40 sand proppant at 1 lb/ft^2
- Sand at 8-10k psi, retains only ~7% to ~2% of baseline conductivity
- Significant loss of conductivity compared with ceramic due to crushing and fines migration issues
- 20/40 Sand (1 lb/ft^2) worse than 0.5 lb/ft^2 of 30/50 Ceramic

Coal fines banking & restricting flow

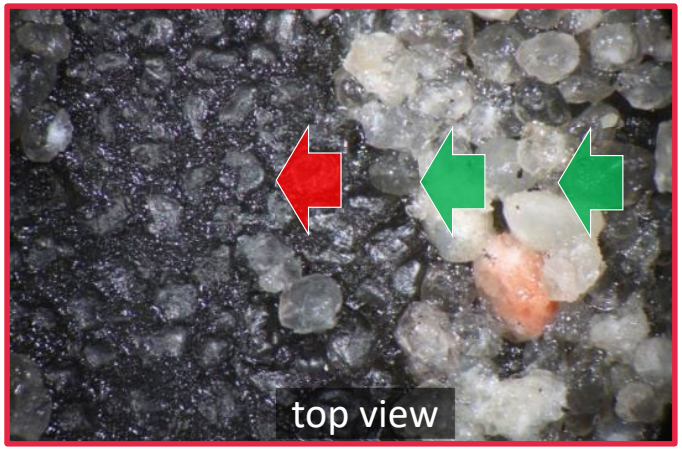

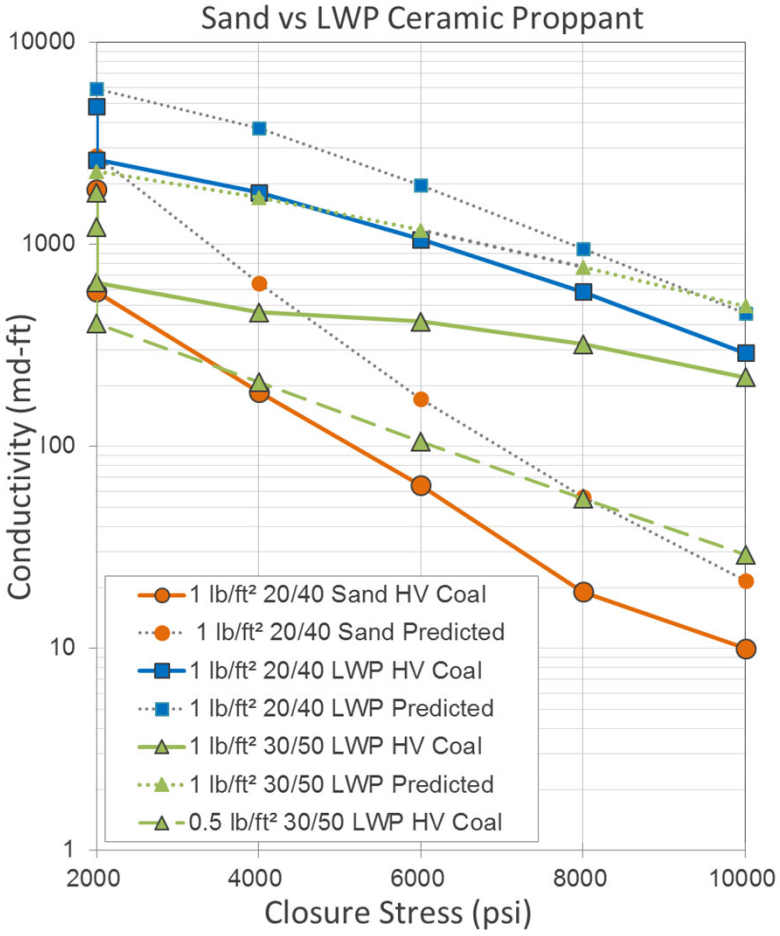

Fraser and Johnson, SPE-191883-MS, 2018

Results – Ceramic conductivity vs coal thermal maturity

- 20/40 cleans up better than 30/50 in HV coal, however Anthracite coal results are almost identical (Fig. 1)
- 20/40 LWP Ceramic retains better conductivity than 30/50 (Fig. 2).
- 30/50 holds down fines to the surface, whereas 20/40 releases fines into the proppant pack (example, Fig. 3 & 4).

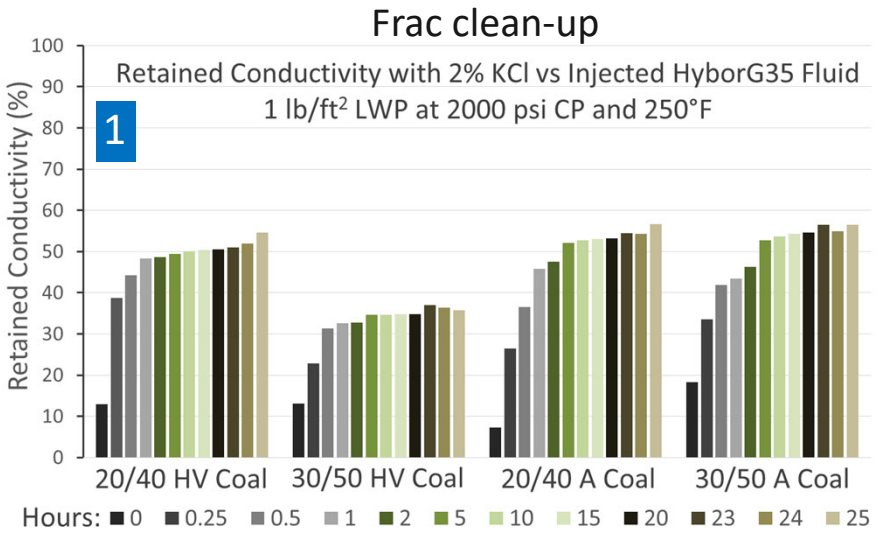

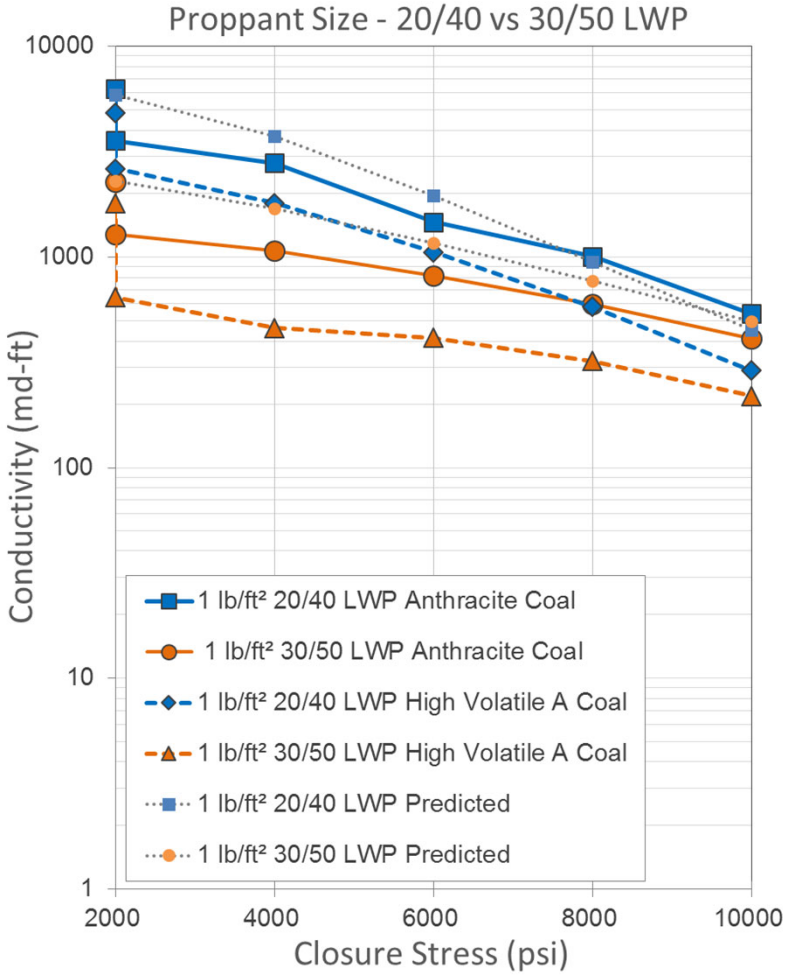

Fraser and Johnson, SPE-191883-MS, 2018

PROPPANT TRANSPORT, STRAINING AND EMBEDMENT BEHAVIOUR (4)

- By applying the LBM-DEM approach (Wang et al., 2018), numerical modelling of suspension transport was studied based on a coal fracture of width W_0 intersecting a cleat of width W_2 based on particle size (d) and volumetric particle concentration (ϕ).
- The results of this modelling indicate that we can explicitly capture particle transport behaviour and the effect of different factors on the leak-off process based on the geometry of the cleat to fracture intersection.
- This was the first iteration of several small-scale transport models that will ultimately be upscaled and applied in the field-scale design of GPI implementation.
- This and further published and unpublished results are consistent with cleat leak off studies performed at StimLab in 1995 to understand hydraulic fracturing damage to coals (Penny & Conway, 1995)

Figure 11: LBM-DEM Transport Model Setup

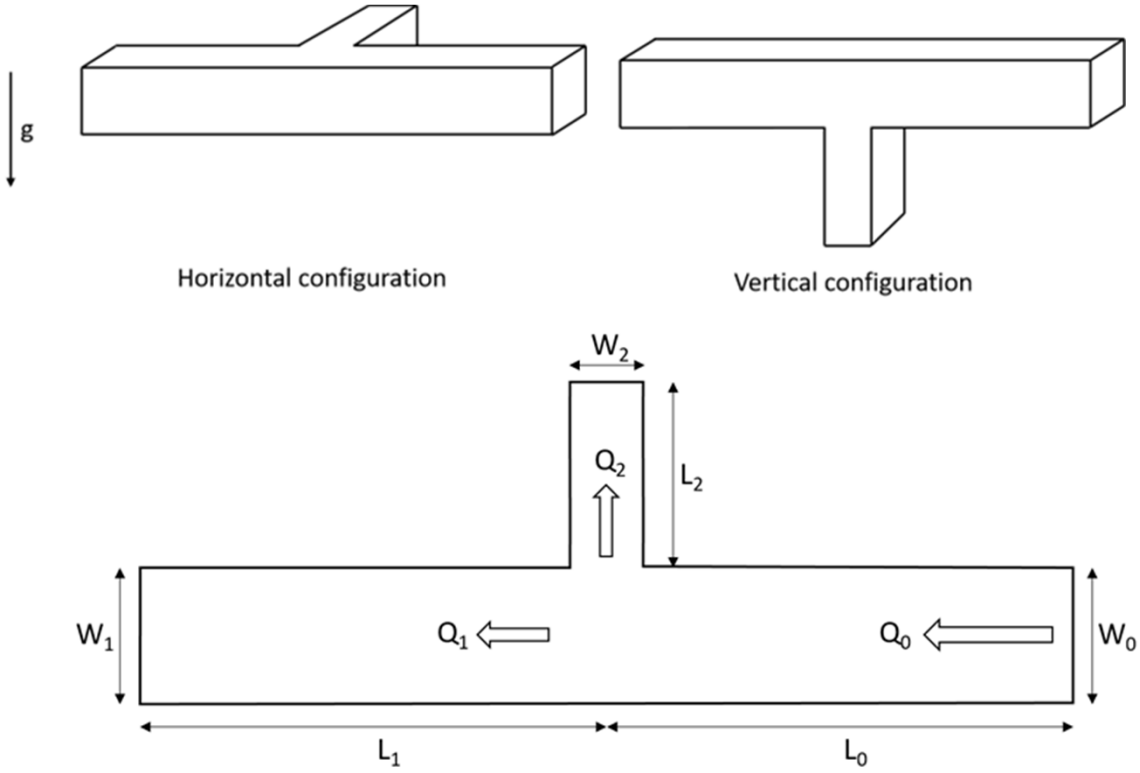

Cross-sectional dimensions

PROPPANT TRANSPORT, STRAINING AND EMBEDMENT BEHAVIOUR (5)

THE UNIVERSITY OF QUEENSLAND AUSTRALIA

Figure 12: LBM-DEM Transport Modelling Results

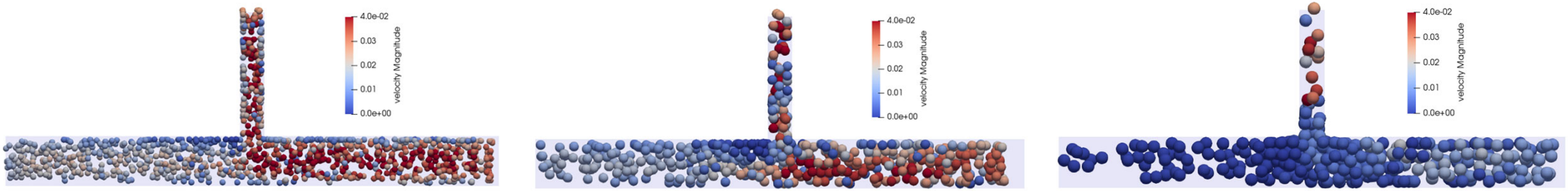

$d/W_2 = 0.25$ $d/W_2 = 0.4$ $d/W_2 = 0.5$

- The effect of particle concentration on the leak-off is investigated by simulations performed for three particle sizes holding $W_0/W_2 = 2$.
- Results indicate that a decrease in particle concentration yields slightly lower leak-off for all sized particles attributed to a reduction in particle accumulation at the junction, as well as reduced transverse particle motion due to reduced particle interactions.
- Further studies have indicated this agglomeration of particles can result in an increased probability of a fracture screen-out (see Di Vaira et al., 2021, 2022)
- **The headline from this modelling is that particles like 100 mesh (~149 microns) will find it impossible to enter cleats and small fractures (10's of microns)**

TRANSPORT, STRAINING AND EMBEDMENT BEHAVIOUR IN GPI (6)

THE UNIVERSITY OF QUEENSLAND AUSTRALIA

Figure 13: StimLab Cleat Leakoff Studies Results

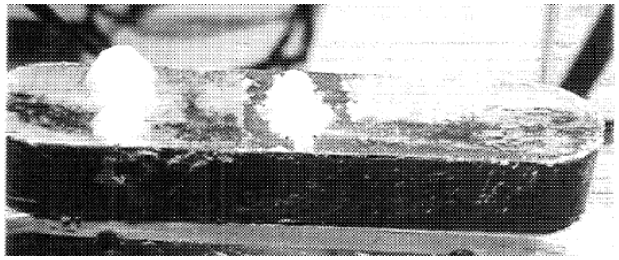

12/20 sand (left) vs 100 Mesh (right) with 40 mD cleat

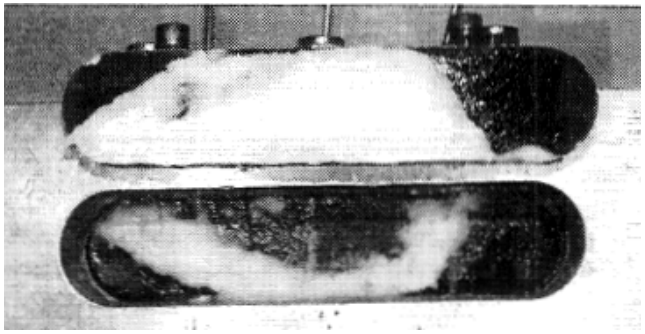

40/70 sand vs 50 and 180 micron cleats

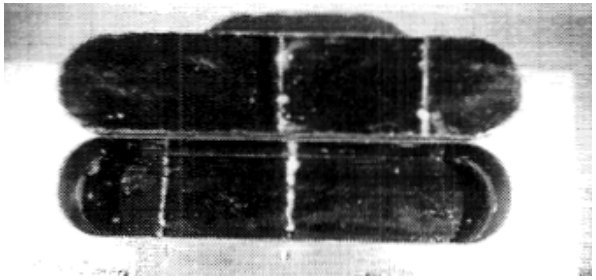

100 and 625 mesh sand vs 120 and 180 micron cleats

- Cleat leak off studies performed at StimLab in 1995 showed increased occlusion into the conductivity cell with increasing mesh size (Source Coordinated Studies in Support of Hydraulic Fracturing of Coalbed Methane, GRI Report, Penny & Conway, 1995)
- **Again… particles like 100 mesh (~149 microns) will find it impossible to enter cleats and small fractures (10's of microns)**

Screen out mechanisms

Figure 14: (a) Probability of screen out, P, obtained at discrete ϕ with the multiple numerical tests at w/d=1.8. The discrete ϕ are predicted with a continuous binomial regression model, from which predicted ϕ at P = 0.05 and 0.95 are obtained. (b) Plotting of P = 0.05 and 0.95 points for a range of w/d. The grey and white regions represent where screen out will and will not occur, respectively, for 5% of cases (Di Vaira et al., AP-URTEC-2021-208342, 2021)

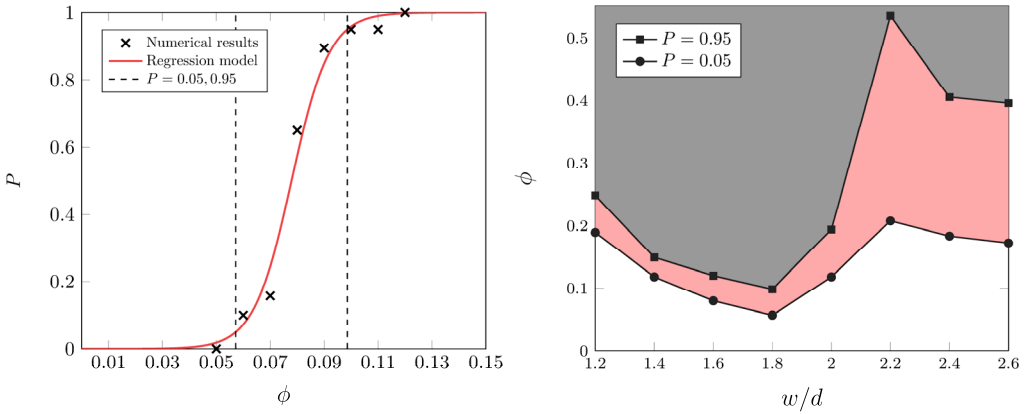

(a) (b)

Figure 15: Example particle agglomeration at screen out conditions without electrostatics

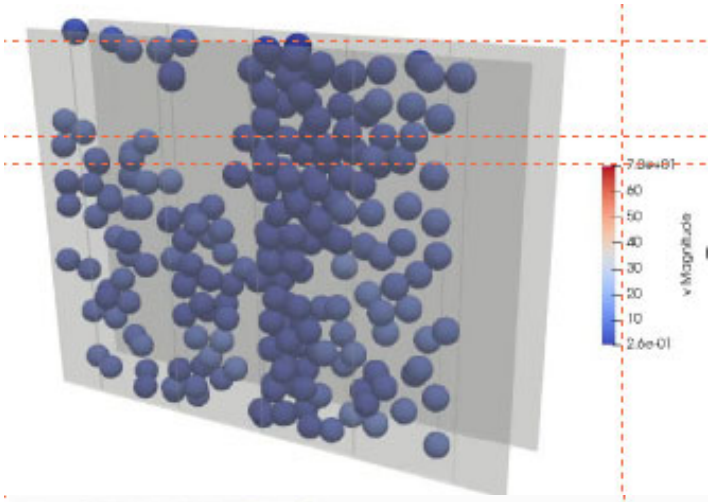

Figure 16: Example particle agglomeration at screen out conditions with electrostatics

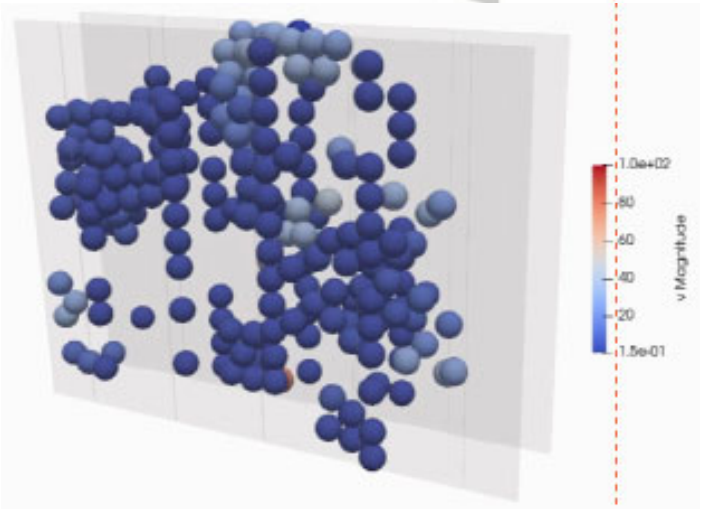

Screen out Mechanisms

Figure 17: Preferential formation of plugs with smallest particles in polydisperse suspensions with Φ ≥ 0.4 Reproduced from Di Vaira et al. (2022).

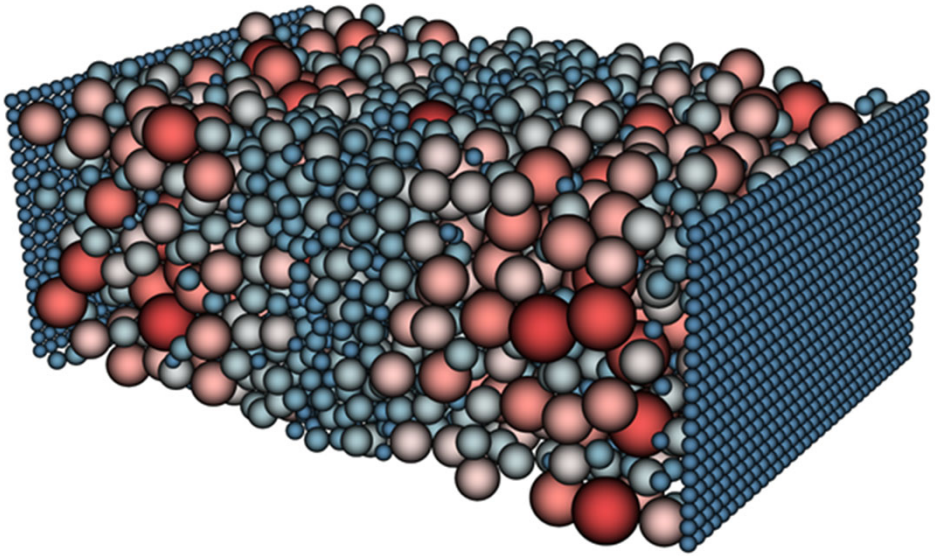

Figure 18: Formation of 40/70 mounds at the intersection of natural fractures and cleats (occluding the fracture and resulting in screen outs)

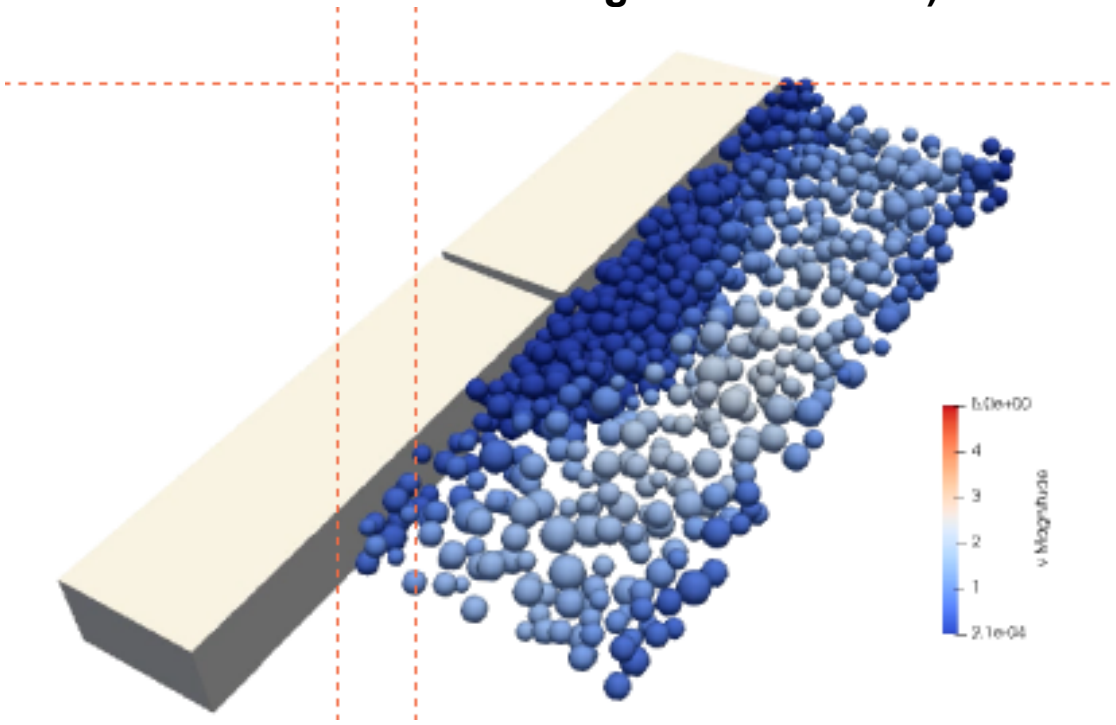

Known techniques to develop initial parameters for PDL Model

- An evaluation of DFIT using before closure (BCA) and after closure analysis (ACA) methods can define stress (Figure 19), pressure dependent leak off (PDL) coefficient (Figure 20), permeability and pressure
- The PDL coefficient predicted for leak off beyond conventional leak off (Howard & Fast, 1957) can be used to history-match observed DFIT pressures in a PDL capable planar 3D fracturing model (Figure 21)

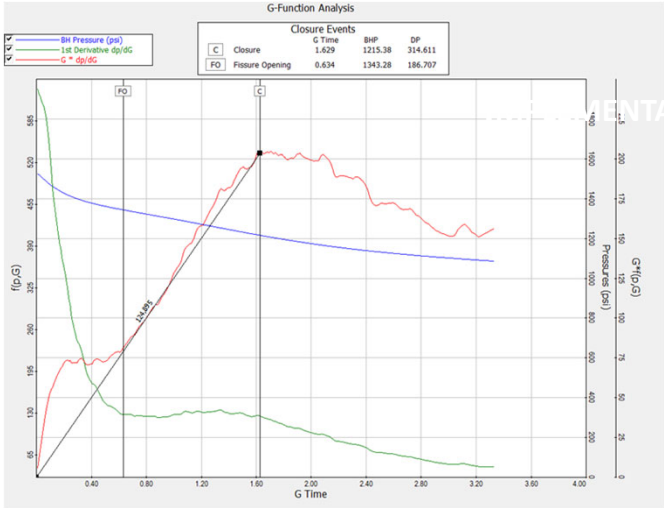

Figure 19: G-Function analysis (Barree, et al., 2002)

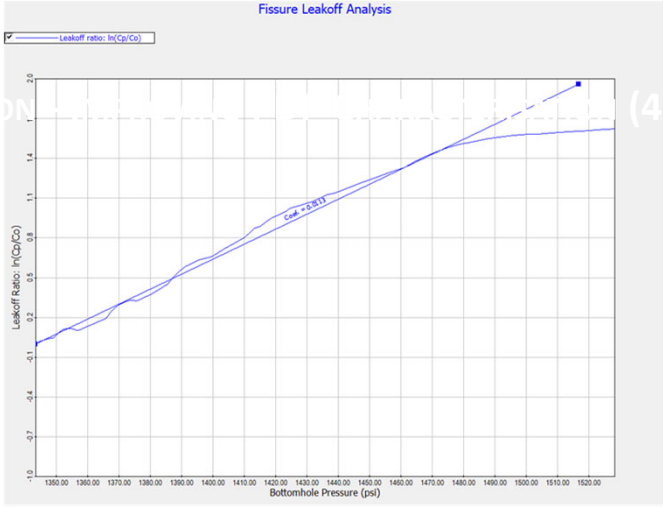

Figure 20: Determination of PDL Coefficient (Barree & Mukherjee, 1996)

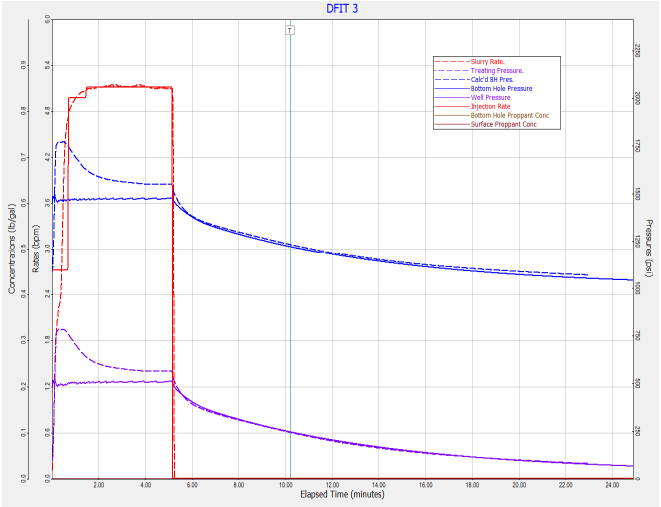

Figure 21: Planar 3D hydraulic fracture model history-match

Integration of PDL to PDP parameters for a reservoir model

Figure 22 Planar 3D or 2D PKN PDL/PDP Integrated Fracture Model

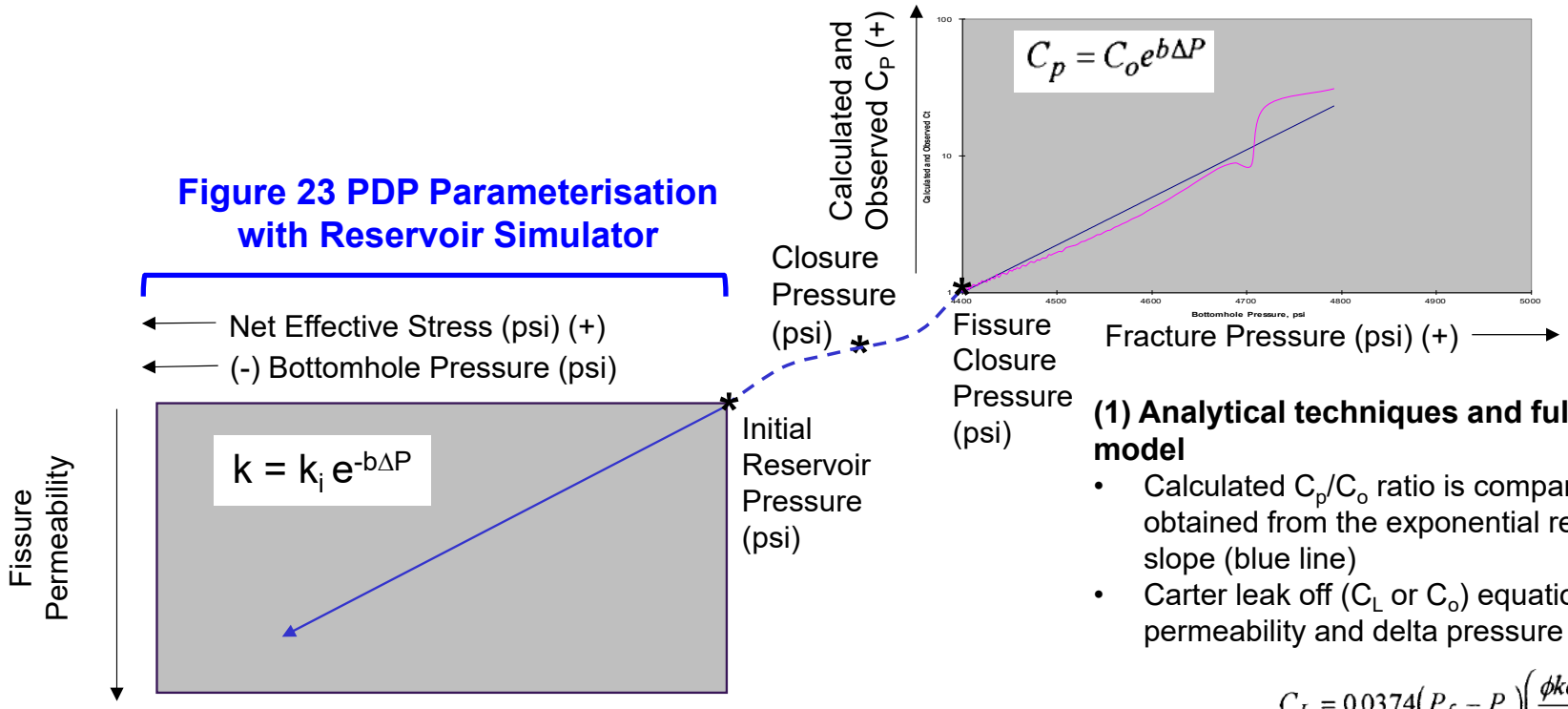

Figure 23 PDP Parameterisation with Reservoir Simulator

(1) Analytical techniques and fully planar 3D frac model

- Calculated C_p/C_o ratio is compared with the value obtained from the exponential relation, where b = slope (blue line)
- Carter leak off (C_L or C_o) equation is driven by permeability and delta pressure

$$C_{L_t} = 0.0374\left(P_f - P_o\right)\left(\frac{\phi k c_t}{\mu}\right)^{0.5}$$

Reservoir model history-match to derive fracture compressibility

- Using a PDP-capable reservoir simulator (PDRS) and multivariate analysis:
  - An optimal fit (red line) to after-closure DFIT pressure decline data (blue line) could be obtained (Figure 24)
  - A sensitivity analysis of fracture compressibility to pressure and permeability evaluated (Figure 25)

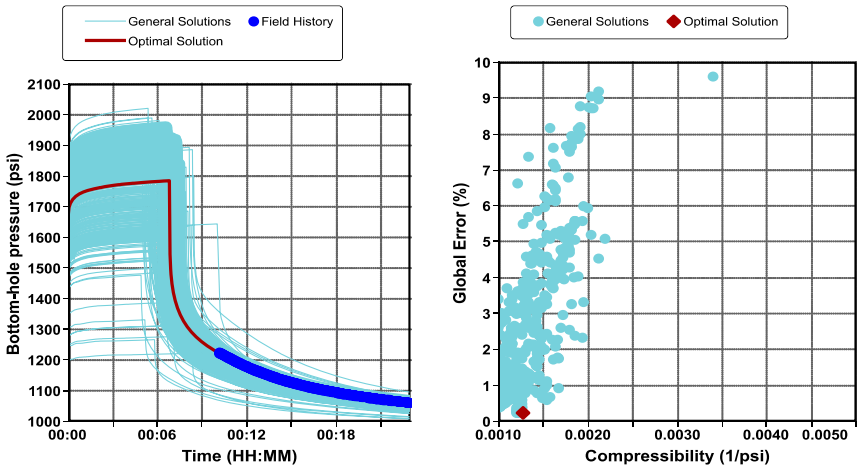

Figure 24: Optimal fit to after-closure DFIT pressure decline data

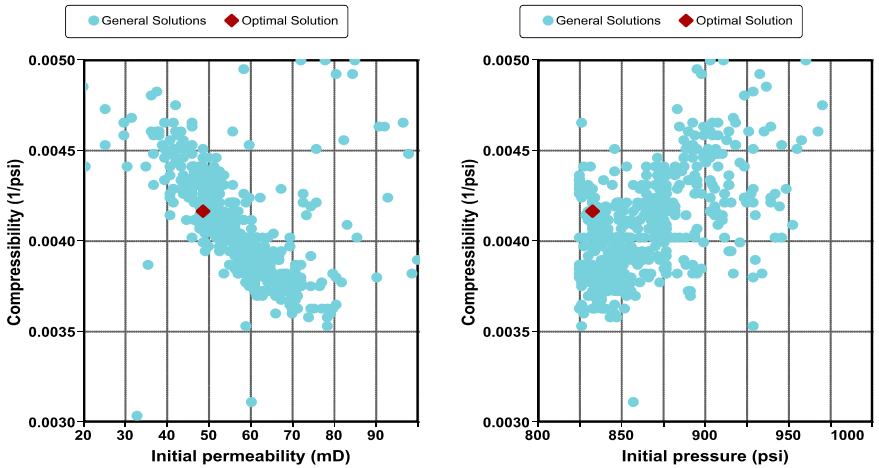

Figure 25: Sensitivity analysis of fracture compressibility to pressure and permeability

IMPLEMENTATION - IMPROVING PDP CHARACTERISATION (4)

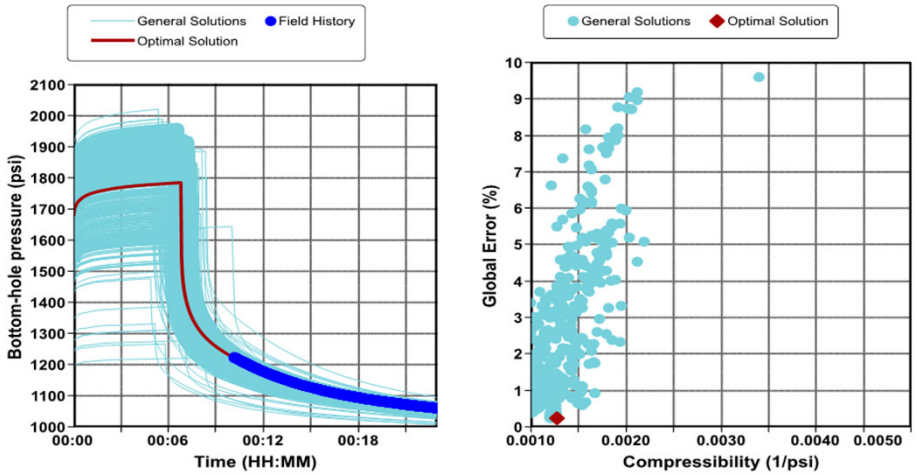

Figure 26

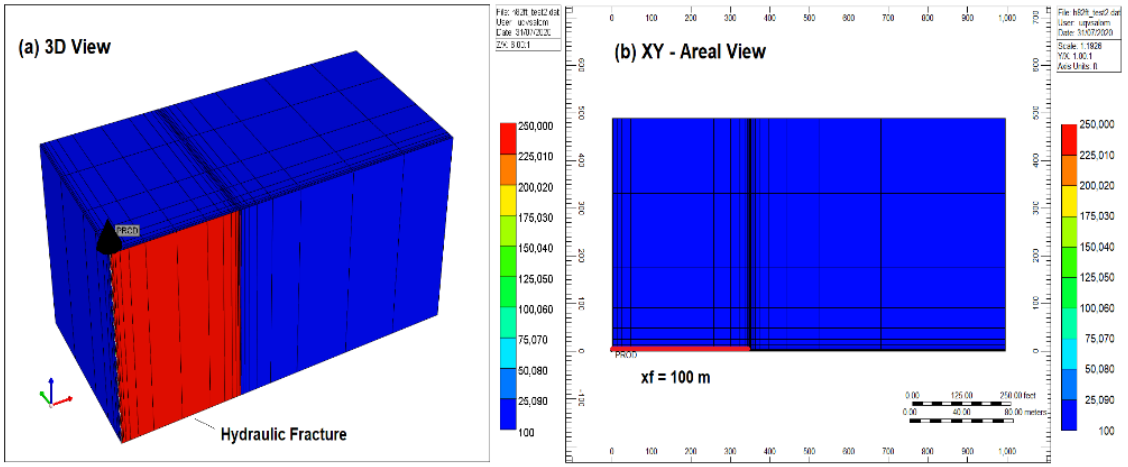

Figure 27

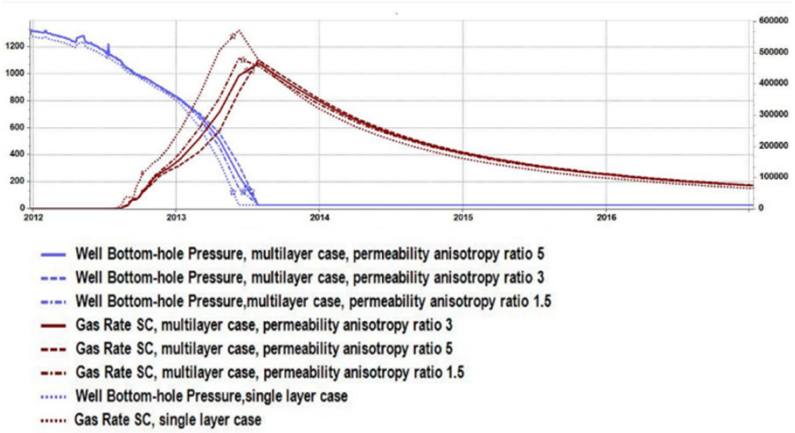

Figure 28

- The permeability, fracture compressibility and PDP parameters derived from history-matching the DFIT decline pressures (Figure 26, using GEM and CMOST) and frac model history-matched estimates of fracture dimensions derived from past diagnostic studies were used to build a GEM model (Figure 27) and history match production– Johnson et al., SPE-202281-MS, 2020
- Further work on anisotropy and multilayer effects explored and model refined (Figure 28)– Ramanandraibe, et. al, AJ20157, APPEA Journal, 2021

MICRO-PROPPANT FOR SRV ENHANCEMENT WITH HYDRAULIC FRACTURING (1)

THE UNIVERSITY OF QUEENSLAND AUSTRALIA

- Multistep simulation procedure previously established for determining SRV permeability increases (Figure 29)
- Calibrated reservoir model with hydraulic fracture modified with an SRV relative to fracture half-length (x_f) in orthogonal direction for coal permeability of 0.1 mD (Figure 30) and 10 mD (Figure 10)
- Next step (1) combine with horizontal multi-stage hydraulic fracture stimulation treatment, optimizing on x_f, lateral length, and number of stages (submitted for APPEA 2022)
- Discussions ongoing with micro-proppant supplier and service provider to deploy on vertical well trial with CNG proponent

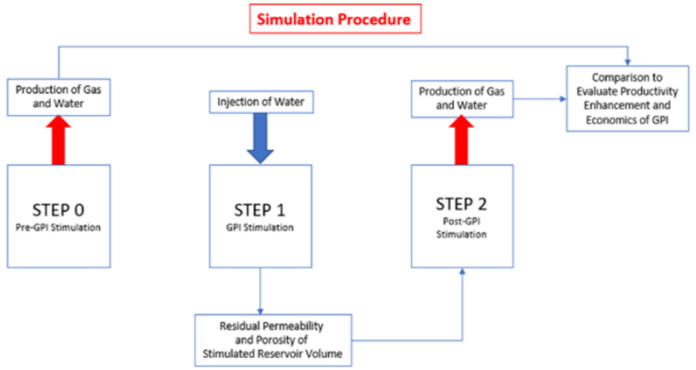

Figure 24 Modified after Ribeiro et al., URTEC-198324-MS, 2019

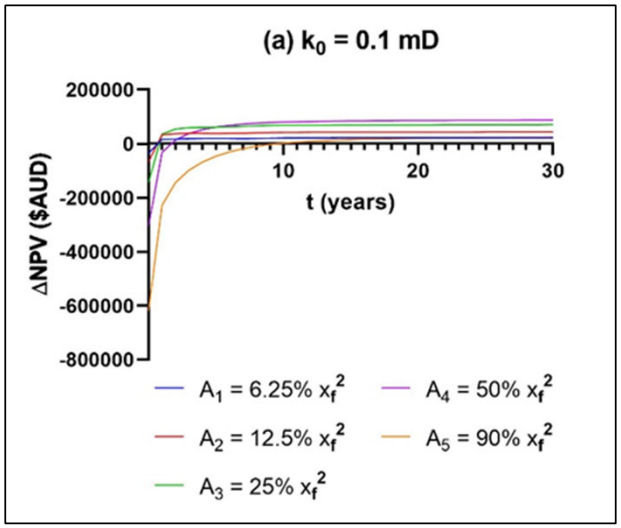

Figure 29

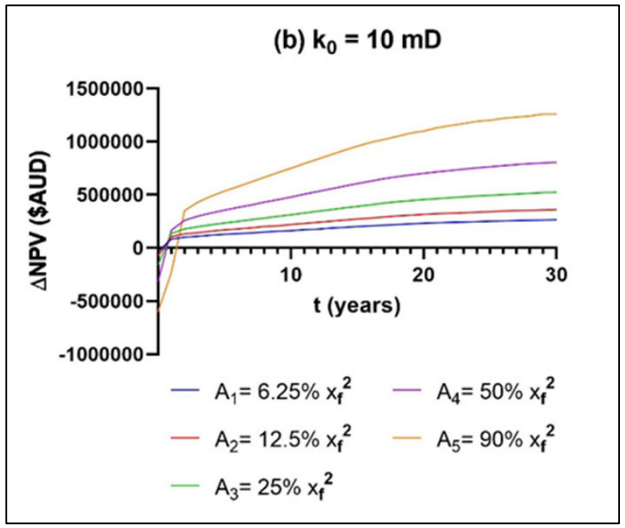

Figure 30

After Santiago, et al., SPE-208404-PA, SPE Journal, 16 Feb 2022

Hydraulic fracture modelling/stress profile/key assumptions

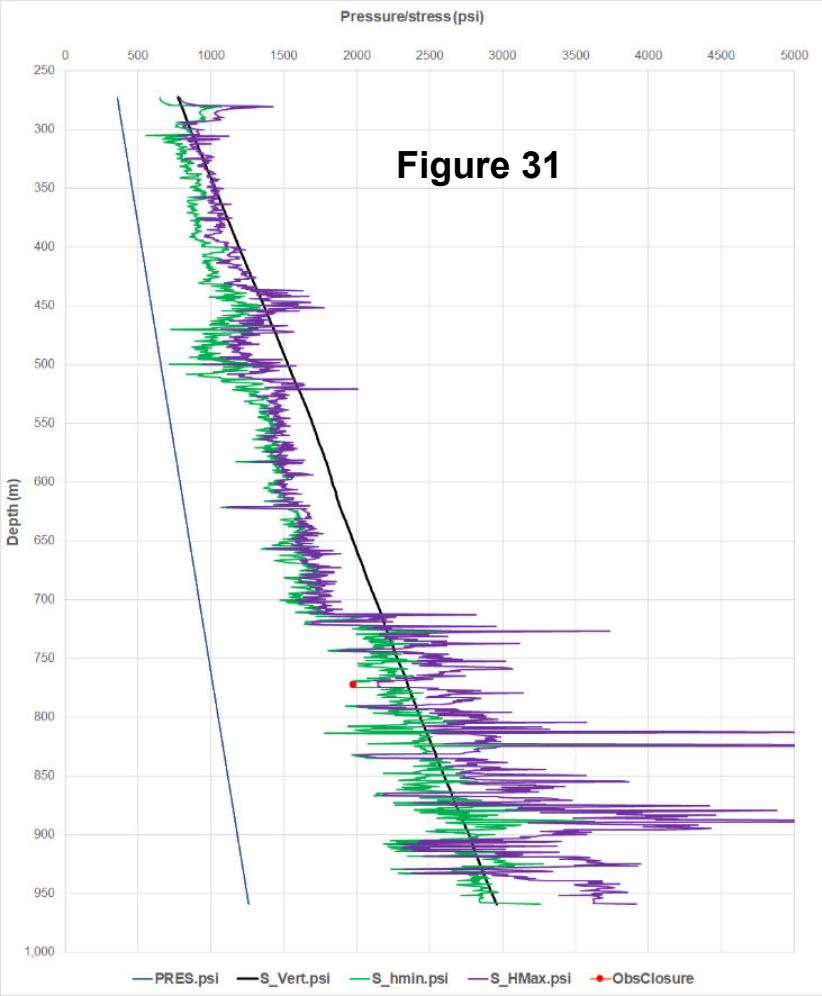

Figure 31

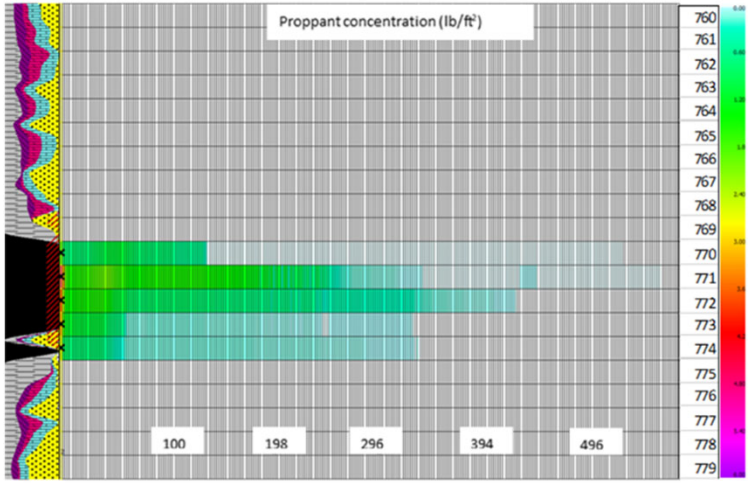

Figure 32

- Closure values, PDL and transverse storage coefficients (b=0.005 psi^{-1}) from Johnson et al. (SPE-77824-MS, 2002)
- Similar fluid and proppant staging in all stages (maintaining wk_f vary x_f)
- Assumed optimal packing of fracture system by micro-proppants (e.g., Keshavarz et al 2104)

*Ramanandraibe, H., Sedaghat, M.,Johnson Jr, R.L, Santiago, V.: "*Co-application of micro-proppant with horizontal well, multi-stage hydraulic fracturing treatments to improve productivity in the Permian Coal Measures, Bowen Basin, Australia", Paper AJ21048, 2022 APPEA Journal.

THE UNIVERSITY OF QUEENSLAND AUSTRALIA

Reservoir modeling inputs consistent with hydraulic fracture design

Parameters (Base case)	Unit	Value
Coal thickness	m	4.6
Porosity	fraction	0.01
Rock compressibility	psi^{-1}	0.00185
Initial matrix pressure	psi	1100
Initial fracture pressure	psi	1120
Permeability I-or x-direction (kx)	mD	1.41
Permeability J- or y-direction (ky)	mD	0.71
Average permeability (k_{avg})	mD	1
Vertical permeability (kv)	mD	0.1
Estimated average hydraulic fracture conductivity	mD.ft	60
Hydraulic fracture permeability (k_f)	mD	1000
Estimated fracture height (H_f)	m	4.6
Estimated fracture half-length (x_f)	m	300
Langmuir volume	m^3/ton	18.63
Langmuir pressure	psi	595
Poisson's Ratio (v)	fraction	0.37
Young's Modulus (E)	psi	500000
Volumetric strain at infinite pressure (ε_∞)	Fraction	0.02676

Figure 36 - 3D view of the Bi-wing fractured reservoir model (red: hydraulic fractured area; blue: naturally fractured area)

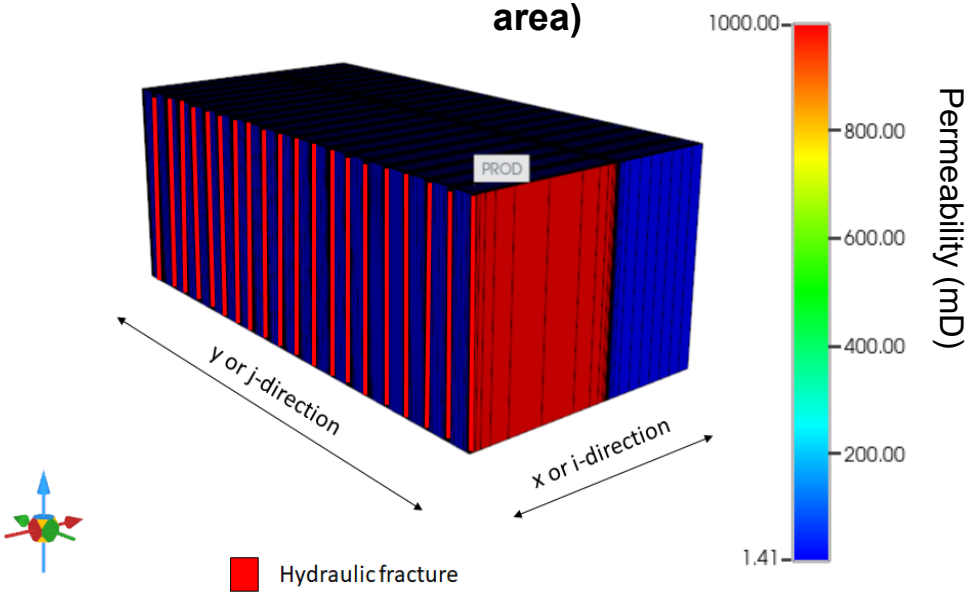

Shrinkage model used for candidate well based on fit of Palmer-Mansoori (SPE-52607-PA) to Burgoyne and Shrivastava (SPE-176834-MS)

*Ramanandraibe, H., Sedaghat, M.,Johnson Jr, R.L, Santiago, V.: "*Co-application of micro-proppant with horizontal well, multi-stage hydraulic fracturing treatments to improve productivity in the Permian Coal Measures, Bowen Basin, Australia", Paper AJ21048, 2022 APPEA Journal.

MICRO-PROPPANT FOR MULTI-STAGE HYDRAULIC FRACTURING (5)

Figure 37 Post-frac and GPI production results (10 mD case)

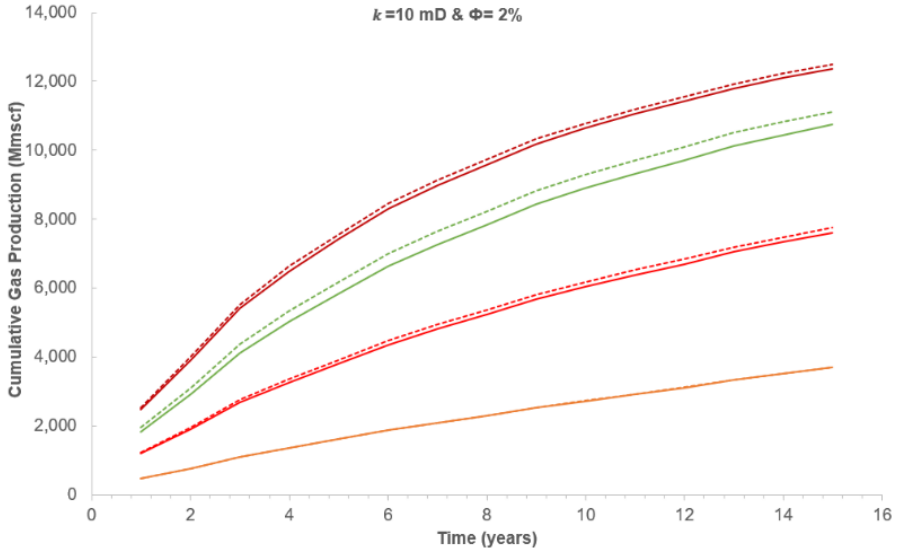

Figure 38 Post-frac and GPI production results (1 mD case)

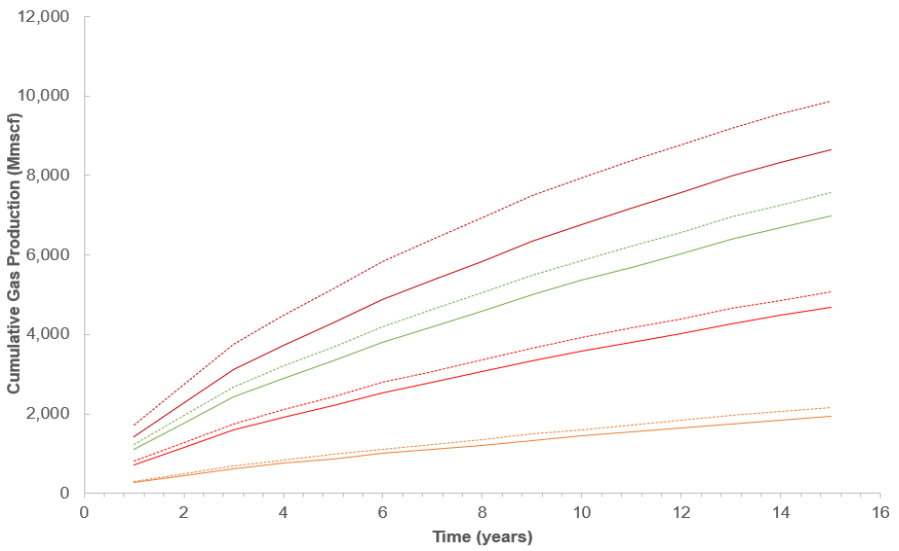

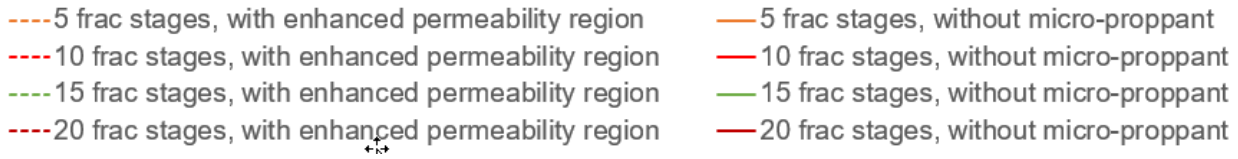

*Ramanandraibe, H., Sedaghat, M.,Johnson Jr, R.L, Santiago, V.: "*Co-application of micro-proppant with horizontal well, multi-stage hydraulic fracturing treatments to improve productivity in the Permian Coal Measures, Bowen Basin, Australia", Paper AJ21048, 2022 APPEA Journal.

MICRO-PROPPANT FOR MULTI-STAGE HYDRAULIC FRACTURING (6)

THE UNIVERSITY OF QUEENSLAND AUSTRALIA

Figure 39 Post-frac and GPI production results (0.1 mD case)

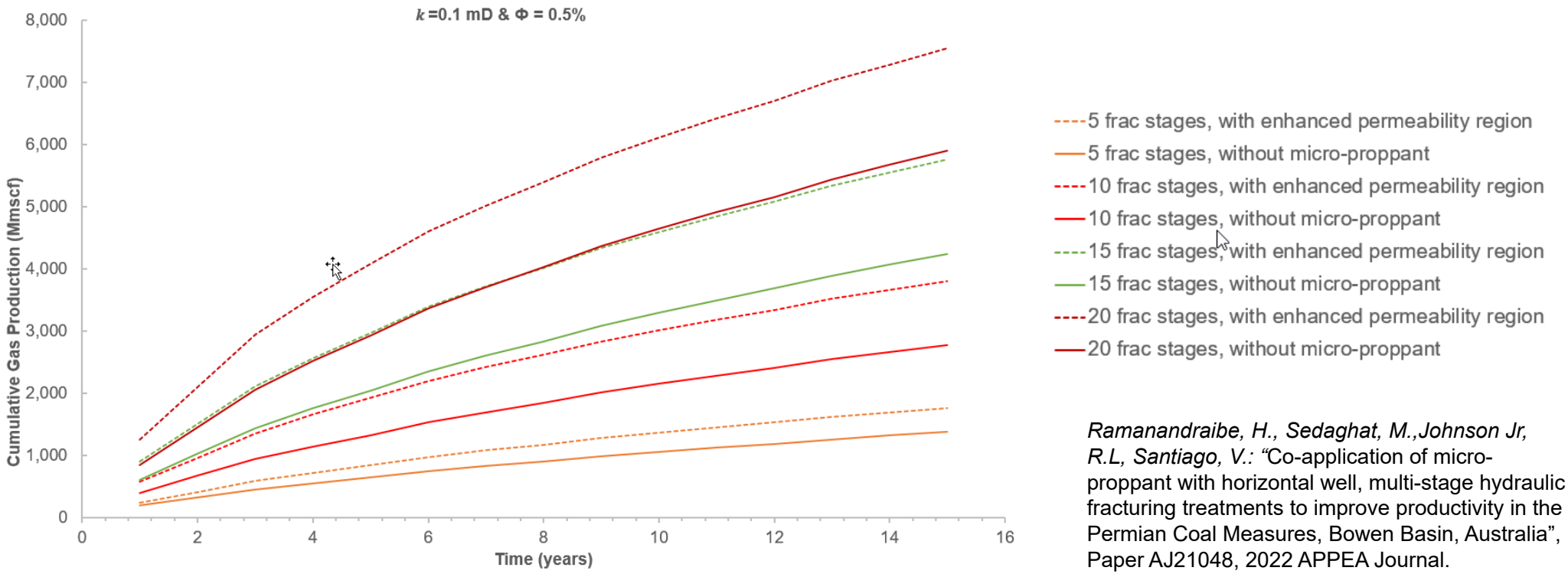

*Ramanandraibe, H., Sedaghat, M.,Johnson Jr, R.L, Santiago, V.: "*Co-application of micro-proppant with horizontal well, multi-stage hydraulic fracturing treatments to improve productivity in the Permian Coal Measures, Bowen Basin, Australia", Paper AJ21048, 2022 APPEA Journal.

	Number of fracture stages							
	5		10		15		20	
	With GPI	Without GPI	With GPI	Without GPI	With GPI	Without GPI	With GPI	Without GPI
EUR (MMSCF)	2162	1944	5070	4682	7560	6985	9868	8656
Recovery factor (%)	11.03%	9.92%	25.86%	23.88%	38.56%	35.63%	50.34%	44.15%

Proppant injection testing – 3D printed fractured media

Figure 40 Design of synthetic rock proposed for a fractured-dominated flow

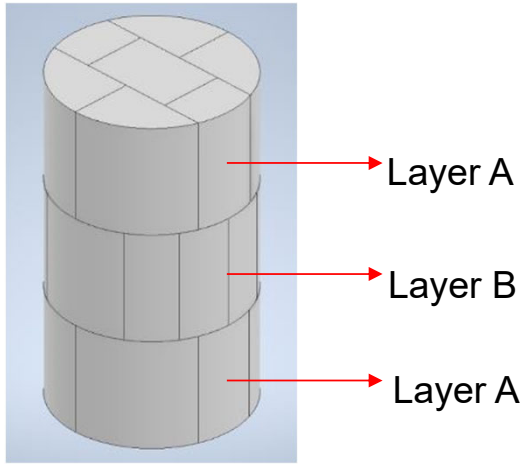

Length: 5 inches
Diameter: 2.5 inches

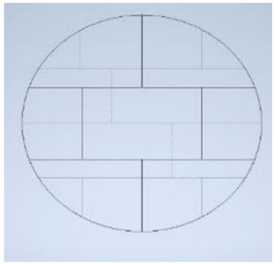

Front

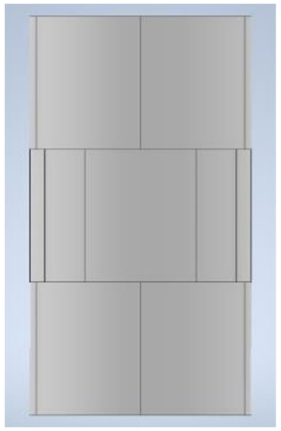

Side

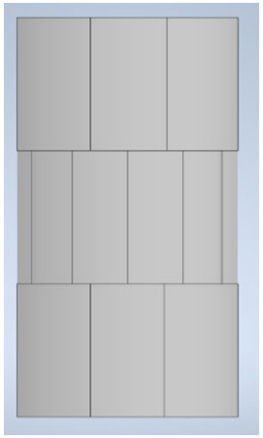

MICRO-PROPPANT EXPERIMENTAL LAB RESULTS (UNIV OF ALBERTA) (2)

THE UNIVERSITY OF QUEENSLAND AUSTRALIA

Figure 41 Proppant injection test 4

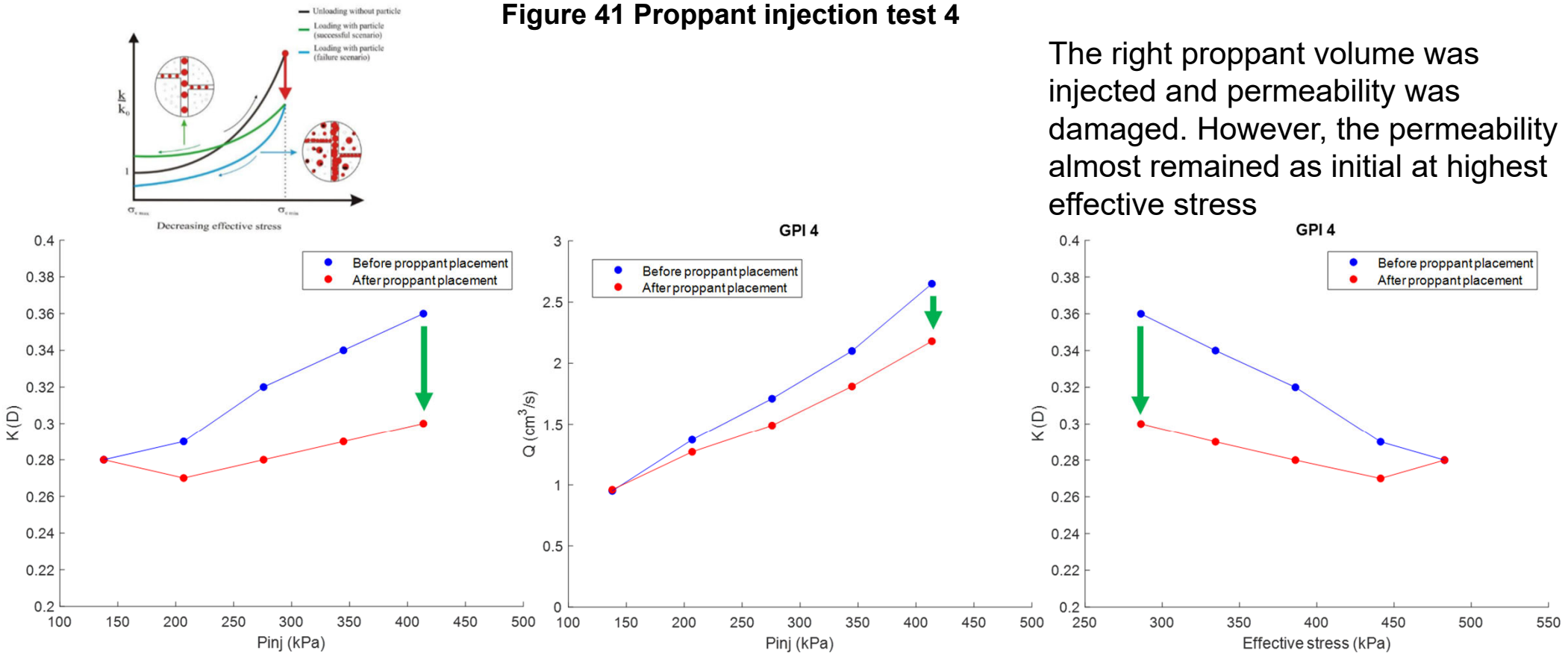

The right proppant volume was injected and permeability was damaged. However, the permeability almost remained as initial at highest effective stress

Disclaimer: The permeability values were calculated with measurements taken from pressure gauges and mechanical devices. It is possible that the differential pressure across the specimen is not entirely accurate.

MICRO-PROPPANT EXPERIMENTAL LAB RESULTS (UNIV OF ALBERTA) (3)

THE UNIVERSITY OF QUEENSLAND AUSTRALIA

Observation of residual proppants inside the synthetic coal after the test

Figure 42

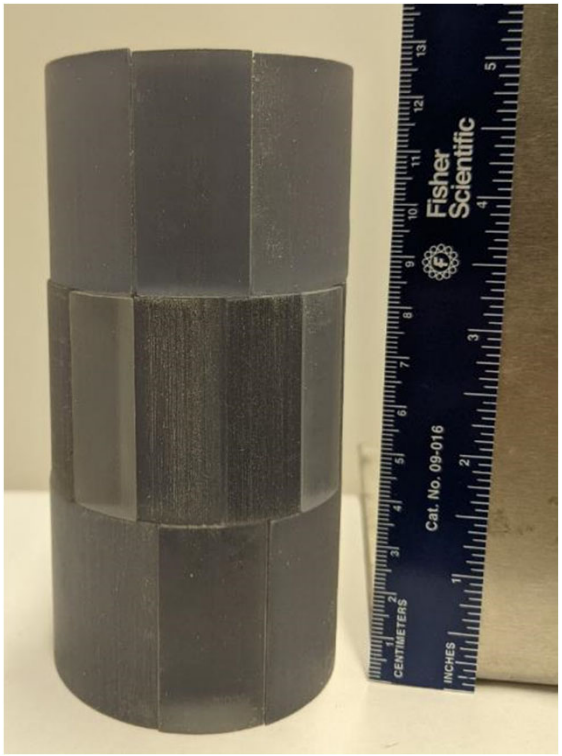

The 3D synthetic core

Micro-proppant between the fractures

Micro-proppant in the drained water

MICRO-PROPPANT EXPERIMENTAL LAB RESULTS (UNIV OF ALBERTA) (4)

THE UNIVERSITY OF QUEENSLAND AUSTRALIA

Observation of residual proppants inside the synthetic coal after the test

Figure 43

Top of the first sample layer

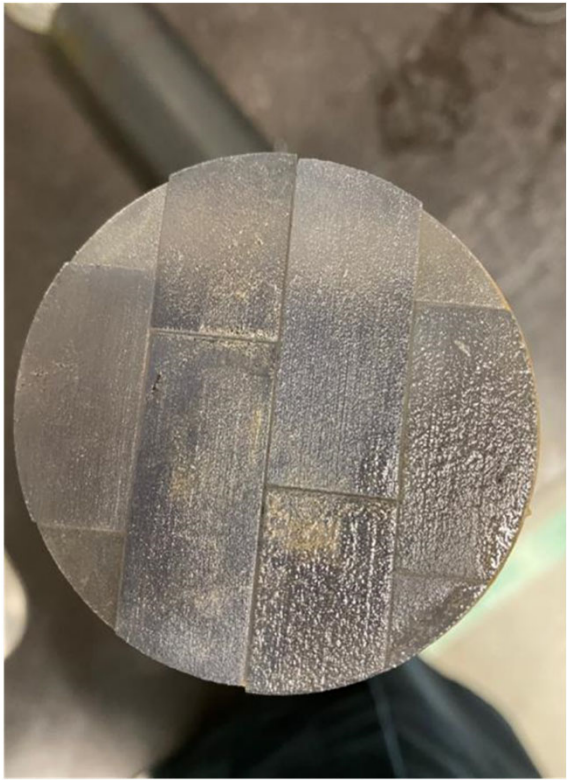

Top of the second sample layer

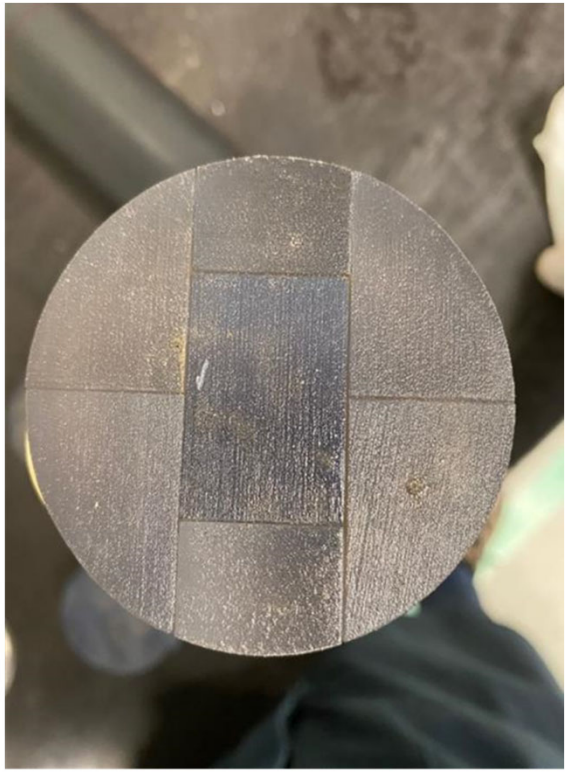

Top of the third sample layer

MICRO-PROPPANT EXPERIMENTAL LAB RESULTS (UNIV OF ADELAIDE) (1)

THE UNIVERSITY OF QUEENSLAND AUSTRALIA

Goals of testing

- Develop a field capable slurry of guar, polymer-specific enzyme and DeepProp 600 particles that would be deployable and diluted 'on-the-fly' with produced water
- Testing with sand packs to ascertain whether DeepProp 600 particles would flow back to the well through a fracture packed with 40/70 or 20/40 proppant (an industry standard) and cause associated problems downstream
- Test with Permian coal sample to ascertain if similar results are possible relative to prior studies by Keshavarz et al.

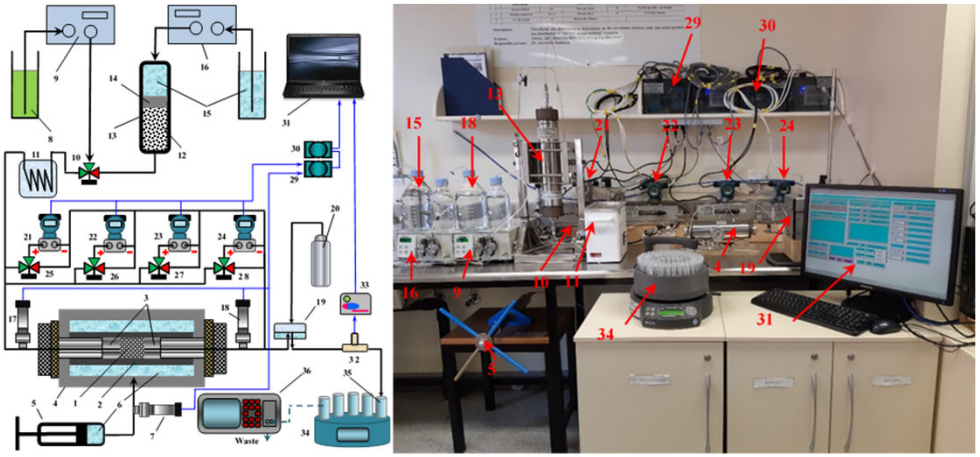

Figure 44: Lab setup and injection schematic similar to field dilution process

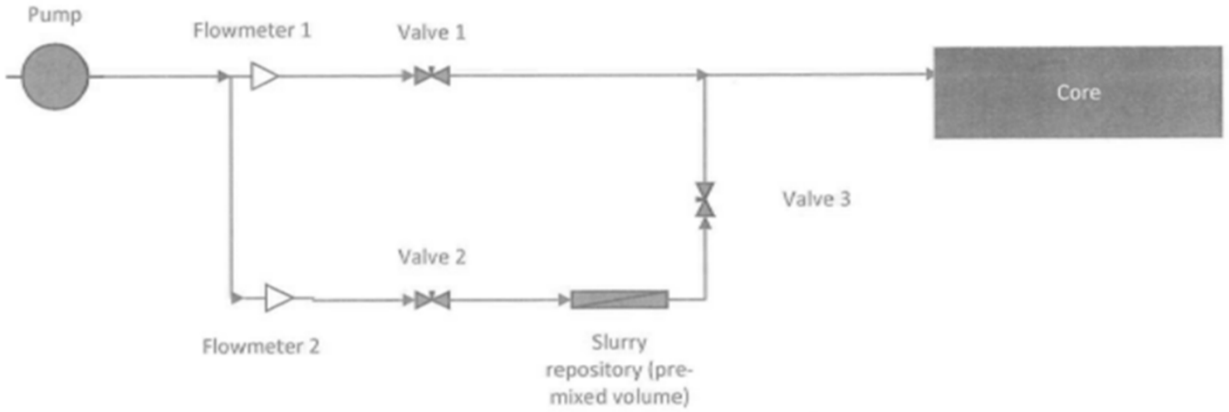

MICRO-PROPPANT EXPERIMENTAL LAB RESULTS (UNIV OF ADELAIDE) (2)

THE UNIVERSITY OF QUEENSLAND AUSTRALIA

Results of testing

- Slurry Preparation: A 80lb/1000 gal guar slurry is capable of suspending 40lb/1000 gal DeepProp 600 particles for dilution 'on-the-fly'
- Sand pack testing at 8 ppg DeepProp 600 loading
  - Particles could not flow back through a fracture packed with 40/70 proppant
  - Testing with a 20/40 sand pack did show a significant reduction of permeability to 335 ± 2 mD (6% retained permeability) from the initial pack permeability of 6045 ± 33 mD and a significant amount of particles in the effluent
  - It is recommended that 100 mesh and 40/70 sand be pumped immediately behind the application of micro-proppants to retain the particles in fractures/cleats as much as is practical.

Figure 45: Examples of guar + DeepProp 600 slurry used in lab testing

Prepared slurry (initial state)

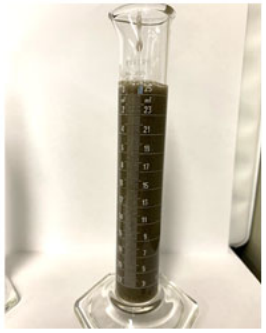

Prepared slurry (1 day after: no separation)

Figure 46: Core flow experiment with DeepProp 600 slurry and 20/40 sand pack

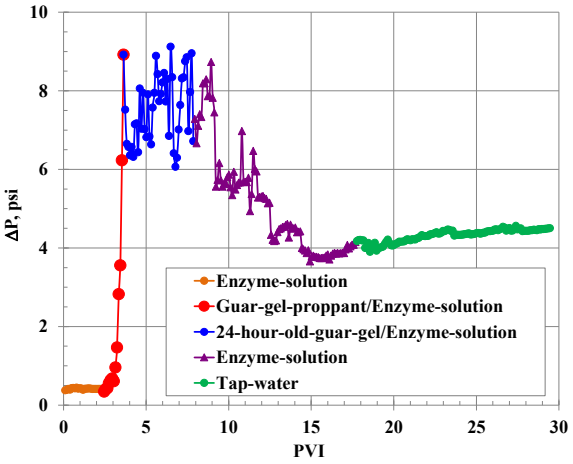

MICRO-PROPPANT EXPERIMENTAL LAB RESULTS (UNIV OF ADELAIDE) (3)

THE UNIVERSITY OF QUEENSLAND AUSTRALIA

Core testing procedure

- Before injection coal cores underwent micro-CT to understand pre-injection distribution and morphology of fractures
- Permeability hysteresis was removed through effective stress loading-unloading
- Additional fractures were generated in this coal core during hysteresis removal procedure, based on pre- and post-CT
- A guar/slurry and enzyme solution mix with 2 ppg equivalent DeeProp 600 loading was injected to a maximum net effective stress (NES) value of 217.6 psi (the laboratory testing constraint established during the hysteresis testing)

Figure 47: Graphs showing removal of hysteresis in reduced core permeability as function of effective stress at 22°C

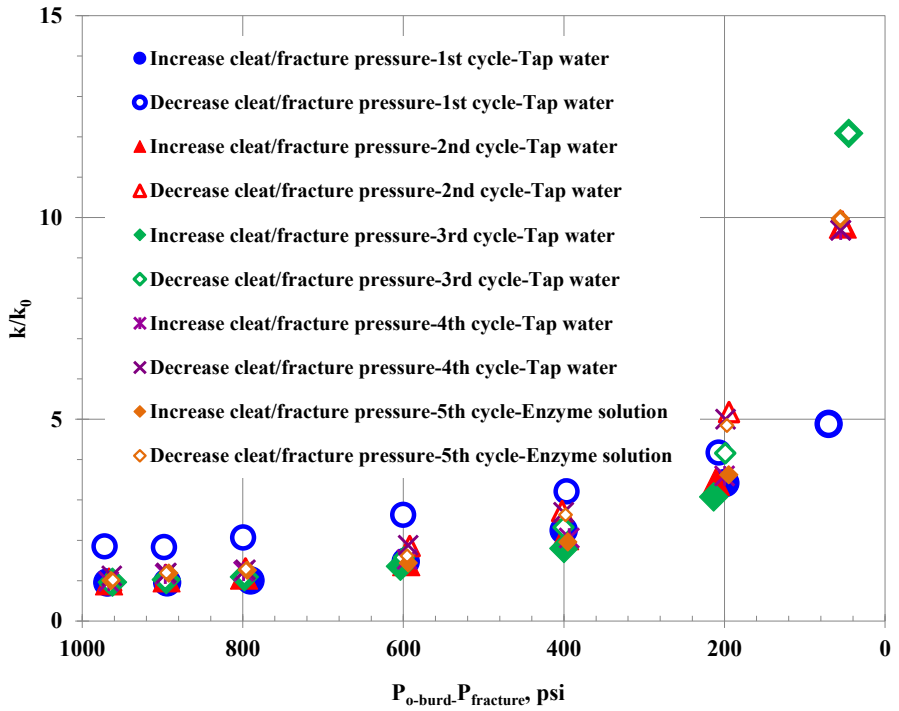

MICRO-PROPPANT EXPERIMENTAL LAB RESULTS (UNIV OF ADELAIDE) (4)

THE UNIVERSITY OF QUEENSLAND AUSTRALIA

Core testing results

- Initially, k/k_o had dropped from 5.14 to 0.023 mD resulting in proppant bridging within the coal core.
- Releasing pressure (increasing NES) the permeability had decreased from an initial value of 18.558 to 1.649 mD.
- Then, after backflushing with enzyme solution, the permeability eventually increased to 2.063 mD
- Thereafter, the permeability decreased likely as a result of fines, proppant movement and fracture closures, as some fractures were filled with micro-proppant
- End result was that under non-fracturing conditions, some damage occurred to the core but recovered likely as a result of self-sorting
- Improvement may be possible under lower NES conditions (i.e., in conjunction with hydraulic fracturing)

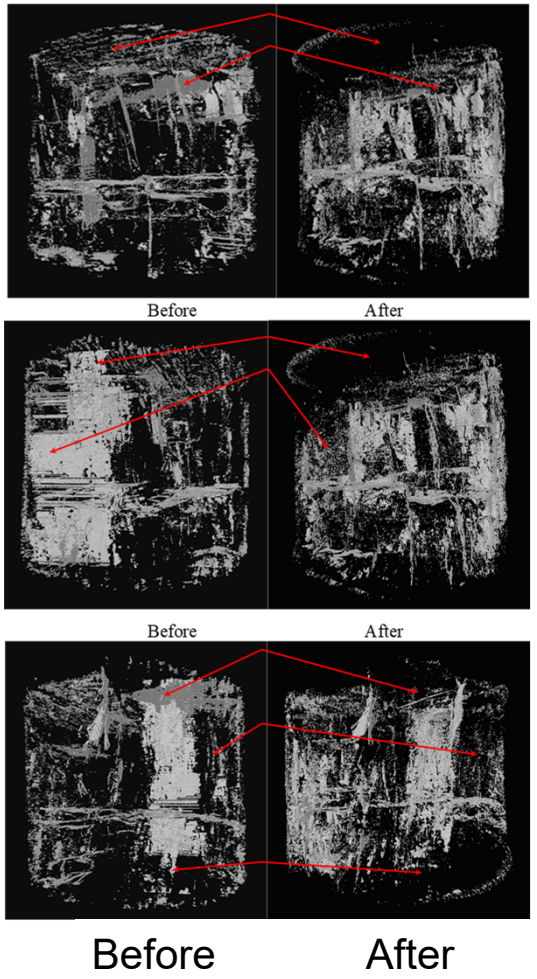

Figure 48: 3D images of pore spaces rotated by 90° for coal core before after proppant deposition.

Summary of Laboratory Testing

- University of Alberta and University of Adelaide testing confirmed slurrying a commercially available micro-proppant in a guar/enzyme carrier was effective and ratio dilution methodology of injection was feasible
- It has increased our understanding on the necessity to correctly match the distribution of particles to the width distribution of cleats and fractures and under fracturing conditions. This was partially successful at high permeability 3D-printed samples (University of Alberta) whereas potential jamming at the interface occurred between the fracture and coal core cleats/fractures (University of Adelaide)
- Further testing is warranted using 3D-printed ‘pseudo-coal’ (i.e., fractured media with rock mechanical properties of coal) and morphologies of expected fracture patterns, based on core or image log analyses.
- Commercial application of silica flour as an intermediate solution may be viable (based on StimLab studies)
- It is recommended that 100 mesh and 40/70 sand be pumped immediately behind the application of micro-proppants to retain the particles in fractures/cleats as much as is practical.

Implementation guidance proposed

- High-level implementation workflow developed including well engineering, geomechanics, hydraulic fracture modelling, required drilling/log data, testing requirements, and reservoir modelling
- More detailed workflows established for field level data acquisition and job execution processes
- Detailed modelling design and evaluation workflows based on examples in the published works of this study

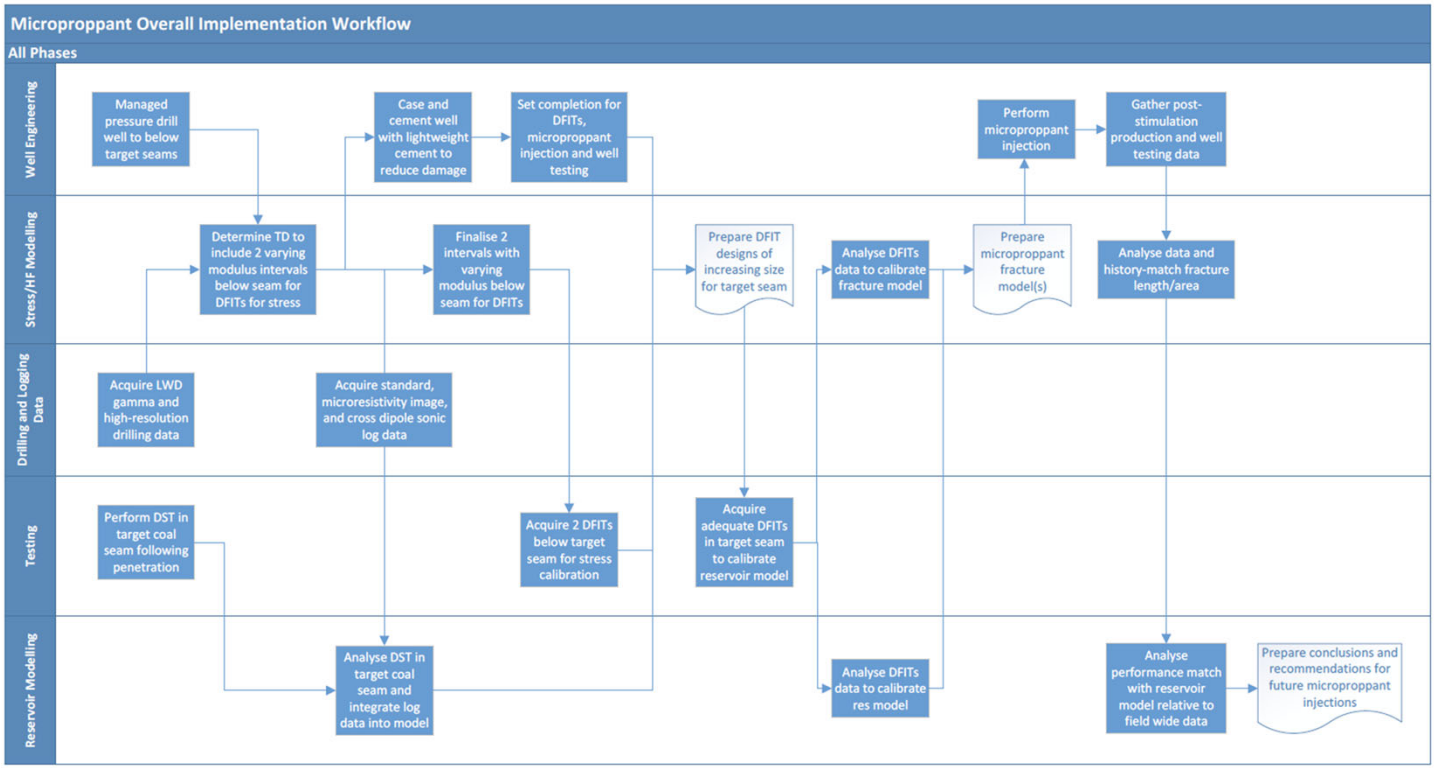

Figure 50: Micro proppant overall implementation workflow

The project aims were achieved..

- Review of hydraulic fracturing models shows a shortcoming in technologies to model complex processes in micro-proppant applications
- Modelling of transport, using the coupled LBM-DEM method, indicates that the micro proppants can be transported deep into formation with a velocity above 3 ft/s (that means smaller profile pumping equipment for standalone applications)
- Embedment modelling indicates that elastic deformation of the coal fracture surface by particles is more pervasive and has impact. Modelled damage and fines generation supported by StimLab proppant coal testing (Fraser and Johnson, 2018)
- New insight on proppant transport and screen out mechanisms match observed data from StimLab studies of the 1990's which found screen outs existing only under limited laboratory conditions (Di Vaira et al., 2022 in progress).

CONCLUSIONS (2)

- A newly developed integrated approach using DFIT data, as well as image log, core analysis, hydraulic fracturing data and production data, can be implemented to reduce uncertainty in the production data analysis and history-matching by consistently incorporating pressure-dependent parameters (Johnson et al., 2020)
- Reservoir modelling including pressure-dependent parameters has been studied for multiple applications (i.e., radial, bi-wing single fracture, and mult-stage horizontal well hydraulic fracturing) with all indicating productivity improvements with the implementation of micro-proppants. Modelling indicates higher folds-of increase with lower permeability coals.
- Laboratory testing was based on principles from 1995 StimLab studies to minimise fluid damage as much as practical with guidelines for ‘on-the-fly’ implementation.
- Report provides series of workflows for design, execution and evaluation of micro-proppant applications based on research

What's needed next?

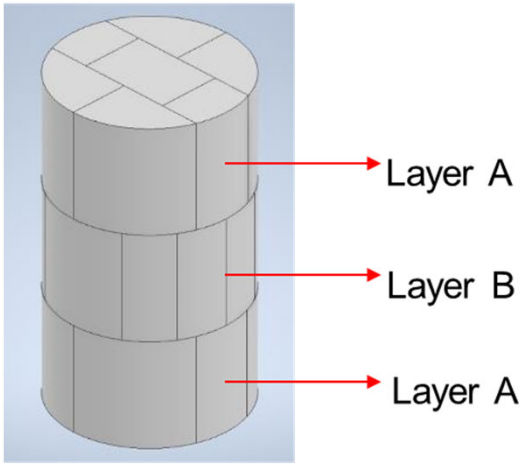

Further testing using 'pseudo-coal' 3D printed samples

Willing candidates!

THE UNIVERSITY OF QUEENSLAND
AUSTRALIA
CREATE CHANGE

Thank you

Prof Raymond Johnson Jr | Professor of Well Engineering and Production Technology
UQ Centre for Natural Gas
r.johnsonjr@uq.edu.au
07 33651234